JVI Journals.ASM.org

Japanese Encephalitis Virus Enters Rat Neuroblastoma Cells via a pH-Dependent, Dynamin and Caveola-Mediated Endocytosis Pathway

Yong-Zhe Zhu,[a] Qing-Qiang Xu,[a] Da-Ge Wu,[a] Hao Ren,[a] Ping Zhao,[a] Wen-Guang Lao,[a] Yan Wang,[a] Qing-Yuan Tao,[a] Xi-Jing Qian,[a] You-Heng Wei,[b] Ming-Mei Cao,[a] and Zhong-Tian Qi[a]

Department of Microbiology, Second Military Medical University, Shanghai Key Laboratory of Medical Biodefense, Shanghai, China,[a] and State Key Laboratory of Genetic Engineering, Institute of Genetics, School of Life Sciences, Fudan University, Shanghai, China[b]

Japanese encephalitis virus (JEV) is a mosquito-borne flavivirus and one of the most common agents of viral encephalitis. The infectious entry process of JEV into host cells remains largely unknown. Here, we present a systemic study concerning the cellular entry mechanism of JEV to B104 rat neuroblastoma cells. It was observed that JEV internalization was inhibited by chloroquine and ammonium chloride, both of which can elevate the pH of acidic organelles. However, JEV entry was not affected by chlorpromazine, overexpression of a dominant-negative form of EPS 15 protein, or silencing of the clathrin heavy chain by small interfering RNA (siRNA). These results suggested that JEV entry depended on the acidic intracellular pH but was independent of clathrin. We found that endocytosis of JEV was dependent on membrane cholesterol and was inhibited by inactivation of caveolin-1 with siRNA or dominant-negative mutants. It was also shown, by using the inhibitor dynasore, the K44A mutant, and specific siRNA, that dynamin was required for JEV entry. Phagocytosis or macropinocytosis did not play a role in JEV internalization. In addition, we showed that JEV entry into the neuroblastoma cells is not virus strain specific by assessing the effect of the pharmacological inhibitors on the internalization of JEV belonging to different genotypes. Taken together, our results demonstrate that JEV enters B104 cells through a dynamin-dependent caveola-mediated uptake with a pH-dependent step, which is distinct from the clathrin-mediated endocytosis used by most flaviviruses.

Japanese encephalitis virus (JEV) is a mosquito-transmitted, enveloped virus belonging to the genus *Flavivirus* within the family *Flaviviridae*, which also includes dengue virus (DENV), West Nile virus (WNV), yellow fever virus, and tick-borne encephalitis virus (26). It is an important human-pathogenic virus, causing approximately 50,000 acute encephalitis cases annually in humans, 25 to 40% of whom will die, with up to 50% of the survivors left with severe residual neurological sequelae (44). JEV has a single-stranded positive-sense RNA genome of approximately 11 kb, encoding a single large polyprotein, which is cleaved by the host- and virus-encoded proteases into three structural proteins, capsid (C), premembrane (PrM), and envelope (E), and seven nonstructural proteins. JEV E glycoprotein is the major structural protein exposed on the surface of the particle and is suggested to be engaged in viral attachment, penetration, and membrane fusion (41). Although a number of cellular components, including glycosaminoglycans (GAGs) (86), laminin (6), and heat shock protein 70 (16), have been shown to participate in JEV infection, the steps that follow the initial attachment of the virus to the candidate receptors are still poorly characterized.

Viruses can utilize several endocytic pathways to enter host cells: macropinocytosis/phagocytosis, clathrin-mediated endocytosis, caveola/cholesterol-dependent uptake, and clathrin- and caveola-independent endocytosis (69). Recent studies have shown that some of these pathways differ only slightly from each other, and certain endocytic components can participate in more than just one pathway (32, 40, 68). Most of the research carried out on flavivirus endocytosis has been done with WNV and DENV. For productive infection of HeLa and SK-N-MC cells, the functional entry of WNV is cholesterol dependent (43), whereas in C6/36 cells, it uses clathrin-mediated endocytosis (12). WNV enters Vero cells by a process that combines features of clathrin and cholesterol endocytosis (10, 42). DENV-1 infection of Vero cells occurs through a classical clathrin-mediated dynamin-dependent endocytosis, while infection of the same cell line by DENV-2 takes place through a nonclassical endocytic pathway independent of clathrin and caveolin-1 but dependent on dynamin (2). This entry route differs from the clathrin-mediated pathway for DENV-2 to infect A549 cells, C6/36 cells (1, 46), HeLa cells (31), and BS-C-1 cells (83). In light of these examples, it is evident that the flavivirus internalization to the mammalian cell is a complex phenomenon wherein a virus of diverse strains may use different mechanisms to enter different cell types.

Upon receptor binding, enveloped viruses exploit two main pathways for internalization of the nucleocapsid into the cytoplasm: (i) membrane fusion at the cell surface (pH independent) or (ii) entry within intracellular vesicles after endocytosis (pH dependent). The conformational changes of the E glycoprotein triggered by the low-pH environment within endosomes during the membrane fusion process of flaviviruses have been studied extensively (47). Recent studies have shown that uptake of JEV virions in C6/36, Vero, and Huh7 cells occurs through receptor-mediated, pH-dependent endocytosis (48, 49, 79). Despite the general consensus about a pH requirement for viral fusion, the information about the precise intracellular pathways for JEV internalization is scanty and controversial. JEV is reported to be

Received 12 April 2012 **Accepted** 20 September 2012
Published ahead of print 26 September 2012
Address correspondence to Ming-Mei Cao, mingmeicao@hotmail.com, or Zhong-Tian Qi, qizt@smmu.edu.cn.
Y.-Z.Z., Q.-Q.X., and D.-G.W. contributed equally to this article.

doi:10.1128/JVI.00903-12

endocytosed to Vero and Huh7 cells, as well as mouse neural stem cells, by a clathrin-dependent, caveolin-independent pathway (17, 49, 79). However, contrasting results have been reported about the role of membrane cholesterol in JEV entry in mouse neuroblastoma cells and BHK-21 cells (34). Recently, we have also shown that JEV enters Huh7 cells in a cholesterol-dependent manner (87).

The aim of this study was to elucidate the internalization mechanism of JEV in B104 rat neuroblastoma cells. We used chemical inhibitors, RNA interference (RNAi) silencing, and the expression of dominant-negative (DN) constructs to examine which cellular molecules are involved in the JEV entry process. The results indicate that JEV endocytosis to B104 cells is dependent on dynamin and caveolae but not clathrin or macropinocytosis.

MATERIALS AND METHODS

Cells and viruses. Cells of the rat neuroblastoma line B104, baby hamster kidney cell line BHK-21, and human embryo kidney cell line 293T were cultured in Dulbecco's modified Eagle's medium (DMEM) containing 10% fetal bovine serum (FBS) (Invitrogen) with penicillin and streptomycin. JEV attenuated strain SA14-14-2 (GenBank accession no. AF315119) was a gift from the Shanghai Institute of Biological Products (SIBP), Shanghai, China. Virus was propagated in BHK-21 cells and titrated by plaque formation in BHK-21 cells.

Kinetics of virus internalization. B104 cells grown in 24-well plates (4.5×10^5 cells/well) were infected with JEV at a multiplicity of infection (MOI) of 0.1 in 500 μl DMEM and incubated at 37°C. At different times, cells were washed with phosphate-buffered saline (PBS) and treated with proteinase K (1 mg/ml) (Invitrogen) for 45 min at 4°C to remove adsorbed but not internalized virus. Proteinase K then was inactivated with 2 mM phenylmethylsulfonyl fluoride (PMSF) in PBS with 3% bovine serum albumin (BSA), and cells were washed with PBS–0.2% BSA by low-speed centrifugation. Finally, pellets were resuspended in DMEM, and different serial dilutions of the cell suspensions were plated onto B104 cell monolayers and overlaid with 1% agarose (SeaPlaque; FMC BioProducts) containing DMEM with 2% FBS. After 3 days of culture, cells were fixed with 10% formaldehyde and stained with 0.5% crystal violet. To determine the rate of virus internalization, a parallel set of cultures was processed under the same conditions, except that proteinase K was replaced by PBS. For each time point, the number of plaques formed in the PBS controls was considered 100%. To separate the adsorption and internalization processes, B104 cells were pretreated with JEV at 4°C for 1 h and then shifted to 37°C. The same experimental procedure was performed as described above.

Virus attachment. B104 cells were grown in 24-well plates and infected with JEV (MOI, 0.1) at 4°C for 1 h. The cells then were washed three times with cold PBS and treated with 1 mg/ml proteinase K for 45 min at 4°C. After treatment, the supernatant was removed and cells were washed three times with cold PBS. Cells were collected in 500 μl of TRIzol reagent (Invitrogen) per well for RNA isolation. RNA from 10^5 cell equivalents was analyzed by reverse transcription (RT)-PCR using a one-step RT-PCR system (Applied Biosystems). Genome copy numbers were normalized to GAPDH (glyceraldehyde-3-phosphate dehydrogenase) gene copy numbers by using the comparative cycle threshold values determined in parallel. Primer sets targeting the 3′-noncoding regions of JEV included forward primer 5′-CCCTCAGAACCGTCTCGGAA-3′ and reverse primer 5′-CTATTCCCAGGTGTCAATATGCTGT-3′. Primer sets targeting GAPDH included forward primer 5′-TGGGCTACACTGAGCAC CAG-3′ and reverse primer 5′-AAGTGGTCGTTGAGGGCAAT-3′.

Production of JEVpv and infection assay. All of the plasmids used for JEV pseudotyped virus (JEVpv) generation were kindly provided by Yoshiharu Matsuura (Osaka University, Japan). Plasmid pCAGVSVG was generated for encoding the G protein of vesicular stomatitis virus (VSV). Plasmid pCAGC105E was generated for encoding of the PrM and E proteins of JEV strain AT31. The JEVpv was generated by a previously described method (79, 80). First, recombinant VSVs were generated. BHK-21 cells expressing T7 RNA polymerase were transfected with 4 μg of mixed plasmids encoding each component of VSV proteins (pBS-N, pBS-P, pBS-L, and pBS-G) and 2 μg of green fluorescent protein (GFP)-expressing plasmid pΔG-GFP using Lipofectamine 2000 (Invitrogen). After 48 h of incubation, the supernatants were inoculated into 293T cells that had been transfected with pCAGVSVG 24 h previously. Recovery of progeny virus was assessed by the appearance of cytopathic effects at 24 to 36 h postinfection. The VSVΔG/GFP-*G recombinant viruses (VSVpv), in which the G gene was replaced with the GFP gene and was pseudotyped with the G protein, were collected. Second, 293T cells transiently expressing the PrM and E proteins of JEV by the transfection with pCAGC105E were infected with VSVΔG/GFP-*G. The virus was adsorbed for 2 h at 37°C and then extensively washed four times with PBS. After 24 h of incubation at 37°C with 10% FBS–DMEM, the culture supernatants were centrifuged to remove cell debris and stored at −80°C. To determine the infectivity of JEVpv, infected cells were identified as GFP-positive cells under fluorescence microscopy or using flow cytometry and expressed as infectious units (IU)/milliliter.

Chemical inhibitors. Monolayers of B104 cells grown in 24-well plates were pretreated with the indicated concentrations of chloroquine, ammonium chloride, chlorpromazine, dynasore, filipin, methyl-β-cyclodextrin (MβCD), genistein, 5-ethyl-*N*-isopropyl amiloride (EIPA), wortmannin (all purchased from Sigma), or okadaic acid (Beyotime Biotechnology, Inc., Jiangsu, China) for 60 min at 37°C. Cell viability upon drug treatment was determined by the cell viability assay (see below). After the treatment, cells were infected with JEV (MOI, 0.1) for 1 h at 37°C and then washed with PBS, treated with proteinase K, and processed as described above. To further determine the entry pathways of the viruses, drug-treated cells were also inoculated with JEVpv and VSVpv.

To assess the effect of chloroquine and ammonium chloride on the pH of acid intracellular vesicles, B104 cells, treated or not with the compound for 1 h at 37°C, were stained with acridine orange (1 mg/ml in DMEM without serum) for 15 min at 37°C. The cells then were washed twice with PBS, mounted on PBS, and visualized on a Zeiss LSM-710 fluorescence microscope.

The function of chlorpromazine, dynasore, filipin, MβCD, EIPA, and wortmannin was confirmed by the uptake of specific endocytic markers. Alexa Fluor 488 (AF 488)-conjugated transferrin (10 μg/ml) (Molecular Probes) was used to control the function of chlorpromazine and dynasore, AF 555-conjugated cholera toxin B (CTB) (10 μg/ml) (Molecular Probes) was used as a control for filipin and MβCD, and Alexa Fluor 555 (AF 555)-conjugated dextran (200 μg/ml; Molecular Probes) was used as a control for EIPA and wortmannin. B104 cells were incubated with the inhibitor for 1 h at 37°C, after which the marker was added. The incubation was continued for 30 min, the cells were fixed and stained with DAPI (4′,6-diamidino-2-phenylindole) (Roche), and the data were analyzed by confocal imaging.

Cholesterol quantification. B104 cells treated with 2.5, 5, 7.5, and 10 mM MβCD were washed with PBS three times and then lysed in lysis buffer (1% Triton X-100, 25 mM HEPES [pH 7.4], 150 mM NaCl, 5 mM $MgCl_2$, 20 μg/ml aprotinin, 10 μg/ml leupeptin, and 1 mM phenylmethylsulfonyl fluoride). Lysates were spun at 10,000 × *g* for 5 min to remove debris, and cholesterol levels were quantitated using an Amplex Red cholesterol assay kit (Molecular Probes) according to the manufacturer's instructions. A standard curve using purified cholesterol was generated for each experiment and normalized to the number of cells.

Transfection of B104 cells. Plasmid constructs expressing GFP-tagged wild-type (WT) and K44A dominant negative (DN) dynamin II were provided by Mark McNiven (Mayo Institute, Rochester, MN) (8). The EPS 15 WT and DN (Δ95/295) constructs, both containing proteins fused to GFP, were kindly provided by A. Benmerah (INSERM, Paris, France) (5). The GFP-tagged constructs expressing wild-type caveolin-1

(GFP-cav-1 WT) and GFP-cav-1 DN mutants were kindly provided by J. M. Bergelson (University of Pennsylvania) (55). Briefly, B104 cells were seeded onto 24-well tissue culture plates and grown overnight until 75% confluence. Next, 0.8 μg of the plasmid construct was complexed with 50 μl of Opti-MEM (Invitrogen) for 5 min at room temperature. The mixture was then added to 50 μl of Opti-MEM containing 2 μl of Lipofectamine 2000 (Invitrogen) that had undergone similar incubation conditions. After a further incubation period of 20 min, the DNA-liposome complexes were added to the cells, which had been starved in Opti-MEM for 4 h before transfection. After incubation for 6 h at 37°C, 1 ml of maintenance medium was added, and the mixture was incubated for a further 48 h before virus infection.

Immunofluorescence assays. B104 cells transfected with plasmids were infected with 0.1 MOI of JEV and incubated for 1 h at 37°C. At 24 h postinfection, cells were fixed with 4% paraformaldehyde for 20 min at room temperature and permeabilized with 0.1% Triton X-100. The cells then were stained with anti-JEV E mouse monoclonal antibody (a gift from The Fourth Military Medical University, Xi'an, China) at room temperature for 1 h. After being washed with PBS three times, the cells were reacted with AF 555-conjugated anti-mouse antibody (Invitrogen). Nuclei were stained with DAPI. The percentage of infection of GFP-expressing cells was calculated by scoring the number of cells positive for viral antigen from approximately 500 transfected cells with comparable levels of GFP expression.

Colocalization of JEV with endocytic markers. B104 cells seeded on coverslips were washed twice with PBS and incubated for 30 min at 4°C with specific endocytic markers (10 μg/ml AF 555-conjugated CTB or 10 μg/ml AF 555-conjugated transferrin) and JEV (MOI, 1). After attachment at 4°C, cells were transferred to 37°C for 1 h to allow the endocytosis of CTB, transferrin, and JEV. Cells were washed twice with PBS and then analyzed by immunofluorescence staining using anti-JEV E mouse monoclonal antibody and AF 488-labeled goat anti-mouse IgG. Nuclei were stained with DAPI. Internalization of CTB, transferrin, and the virus was analyzed by confocal microscopy with a 63× objective (Zeiss).

To further study the pathway of JEV entry, virus attachment was permitted as described above and virus internalization was allowed at 37°C for 1 h. Cells were washed, fixed, and stained as described above with anti-JEV E antibody and anti-caveolin-1 antibody (Abcam), followed by fluorescent-labeled secondary antibodies. Nuclei were counterstained with DAPI. Cells were observed using a confocal fluorescence microscope.

siRNA knockdown. Pooled validated siRNAs targeting vacuolar ATPase (VATPase) (catalog no. M-096966-00), dynamin II (catalog no. M-080140-00), clathrin heavy chain (catalog no. M-090659-00), caveolin-1 (catalog no. M-093600-00), and phosphatidylinositol 3-kinase (PI3K) (catalog no. M-095688-00) were purchased from Dharmacon. Nontargeting siRNA (catalog no. D-001206-13) was used as a negative control, whereas siGLO (Dharmacon) acted as a transfection marker. Cells were transfected using Lipofectamine 2000 (Invitrogen) according to the manufacturer's instructions. At 48 h posttransfection, cells were inoculated with JEV or JEVpv. Knockdown efficiencies were quantified by Western blot analysis.

Western blot analysis. Whole-cell lysates from siRNA-transfected B104 cells were generated by adding 2× SDS-PAGE sample buffer to cells. Samples were boiled for 5 min and separated by SDS-PAGE. Proteins were then transferred to polyvinylidene difluoride (PVDF) membranes (Bio-Rad). Membranes were blocked in 5% nonfat milk and incubated with primary antibodies, followed by horseradish peroxidase (HRP)-conjugated antibodies (Santa Cruz Biotechnology). The following antibodies were used: VATPase (Santa Cruz Biotechnology), clathrin heavy chain (BD Transduction Laboratories), caveolin-1 (Sigma), dynamin II (Abcam), PI3K (Cell Signaling Technology), and β-actin (Santa Cruz Biotechnology). Bound antibodies were detected with the ECL Plus enhanced chemiluminescence Western blotting detection reagents (PerkinElmer Life Sciences).

Cell viability. Cell viability upon siRNA transfection and drug treatments was assessed by employing the 3-(4, 5-dimethylthiazol-2-yl)-2,5 diphenyl tetrazolium bromide (MTT) assay (Chemicon International) according to the manufacturer's recommendations. Briefly, B104 cells were seeded in 96-well cell culture plates and subsequently treated with individual siRNAs or drugs for 48 h and 1 h, respectively, before incubation with AB solution for 4 h at 37°C. After this, solution C containing isopropyl alcohol-HCl was added, and the plates were subjected to absorbance reading by an enzyme-linked immunosorbent assay (ELISA) plate reader (Bio-Rad) at a test wavelength of 570 nm and reference wavelength of 630 nm.

Statistics. Student's *t* test was used to determine statistical significance. All graphs represent means and standard deviations of normalized data points for triplicate samples from each of three independent experiments ($n = 9$).

RESULTS

Kinetics and rate of JEV internalization. To define accurately the conditions of the viral internalization assay required for monitoring JEV entry under different treatments, we modified a proteinase K infectious assay published for DENV that determines the kinetics and rate of virus penetration by measuring productive internalized virus particles (2). B104 cells were infected with JEV at 37°C. At the indicated time points after infection, proteinase K was added to remove adsorbed virus, whereas internalized virus remained protected inside the cell; after inactivation of the enzyme, suspensions of infected cells were plated on B104 cell monolayers to quantify infectious internalized particles by plaque formation. As a control, cells were incubated with PBS instead of proteinase K at the indicated times after infection, and a similar infectious center assay was performed to quantify total cell-associated virus (membrane-bound and internalized virions). The percentage of PFU resistant to proteinase K treatment in comparison with control PBS treatment was calculated for each time point. As shown in Fig. 1A, at the beginning of infection, most JEV particles were detached from cells by proteinase K. After 60 min of incubation, 95% of virus was resistant to proteinase K treatment in comparison to control treatment, indicating a successful internalization of infectious virions.

To directly measure the effectiveness of proteinase K treatment, the amount of bound virus was measured by determining the JEV genome copy numbers by quantitative RT-PCR (qRT-PCR). As shown in Fig. 1B, proteinase K treatment significantly affected the number of attached virions at the cell surface, suggesting that proteinase K treatment removes virus attached to the cells.

To separate adsorption and internalization processes, B104 cells were incubated with the virus at 4°C for 1 h to allow virus attachment and then shifted to 37°C to permit virus internalization. At different times after the shift, the amount of internalized virus particles was determined by proteinase K treatment and the infectious center assay as described above. The kinetics and rate of JEV internalization in these assay conditions were comparable to those obtained without 1 h of preincubation at 4°C (Fig. 1C), suggesting the specific effect of proteinase K on virus internalization. Thus, the effect of inhibitors on virus internalization was measured by protease treatment and the infectious center assay after 1 h of JEV infection at 37°C.

JEV entry into rat neuroblastoma cells is dependent on acidic pH. To test whether JEV entry to B104 cells is pH dependent, we first evaluated the effect of two known inhibitors: chloroquine, an endosomal acidification inhibitor (72), and ammonium chloride,

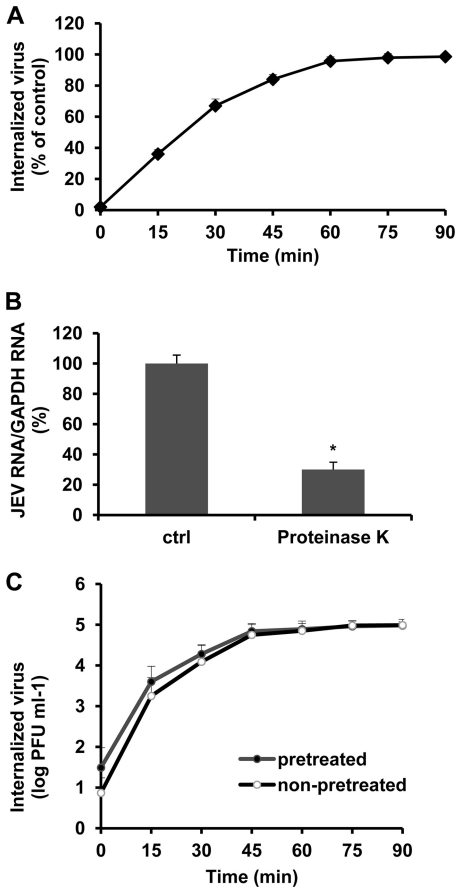

FIG 1 Kinetics and rate of JEV internalization into B104 cells. (A) B104 cells were infected with JEV at 37°C. At the indicated time points after infection, extracellular virus was inactivated with proteinase K. Results are shown as a percentage of internalized viruses compared with controls (ctrl) in which PBS was substituted for proteinase K and are presented as the means ± standard deviations (SD) of three independent experiments. (B) B104 cells were incubated with JEV at 4°C for 1 h, after which the unbound virus was removed and then treated with proteinase K for 45 min at 4°C. Cells were collected in TRIzol for RNA isolation and JEV RNA copy number determination. Results are shown as a percentage of JEV RNA copy number compared with controls in which PBS was substituted for proteinase K and are presented as the means ± SD of three independent experiments. (C) B104 cells were infected with JEV at 37°C (nonpretreated infection) or at 4°C and then transferred to 37°C (pretreated infection). At the indicated times, extracellular virus was inactivated with proteinase K. Results are expressed as number of internalized PFU and are presented as the means ± SD of three independent experiments. *, $P < 0.05$.

a lysosomotropic weak base that immediately raises the pH of intracellular acidic vesicles (45). Pretreatment of B104 cells with increasing concentrations of chloroquine (Fig. 2A) or ammonium chloride (Fig. 2B) revealed significant dose-dependent inhibition of JEV internalization. Possible drug-induced cytotoxic effects were assessed by MTT cell viability assays. Minimal cellular cytotoxicity was observed in drug-treated cells throughout the spectra of concentrations (Fig. 2A and B).

We utilized the pseudotype JEV (JEVpv) system to further test the involvement of acidic pH in the entry of JEV. Single-life-cycle JEVpv contains JEV E glycoprotein and has been used to address the molecular mechanisms of JEV entry into cells (79). B104 cells were pretreated with various concentrations of the inhibitors described above, and then the cells were inoculated with JEVpv and pseudotype vesicular stomatitis virus (VSVpv). As expected, either chloroquine (Fig. 2C) or ammonium chloride (Fig. 2D) strongly inhibited the infectivity of VSVpv, which enters cells through pH-dependent endocytosis (77). Similarly, infection with JEVpv was clearly inhibited by treatment with chloroquine (Fig. 2C) or ammonium chloride (Fig. 2D) in a dose-dependent manner. To ensure that the inhibitors used effectively increased the pH of intracellular vesicles in B104 cells, acridine orange staining was performed. Untreated cells showed the typical cytoplasmatic orange fluorescence of the acid compartments, whereas cells treated with chloroquine and ammonium chloride did not exhibit this fluorescence pattern (Fig. 2E).

Next, we examine the requirement of low pH for JEV entry by silencing the gene encoding vacuolar ATPase (VATPase), a proton pump key to establishing the low pH of endosomal compartments (50). B104 cells were transfected with small interfering RNA (siRNA) targeting VATPase (siVATPase) or control siRNA and then challenged with JEV, JEVpv, or VSVpv. Treatment of B104 cells with siVATPase did not appear to exhibit a cytotoxic effect (Fig. 2F). As shown in Fig. 2F, treatment of siVATPase drastically reduced the amount of internalized virus. Significant decreases in JEVpv and VSVpv infection were also observed in siVATPase-treated cells (Fig. 2G), confirming the requirement for low pH in JEV entry into B104 cells. In addition, efficiency of siRNA-mediated knockdown of VATPase in B104 cells was analyzed by Western blot analysis (Fig. 2H). Taken together, these data demonstrate that JEV enters rat neuroblastoma cells in a pH-dependent manner.

Clathrin is not required for JEV entry into rat neuroblastoma cells. Endosomal acidification is often linked to clathrin-mediated endocytosis (56). In addition, JEV has been shown to exploit the clathrin-mediated pathway to enter Vero cells (49), Huh7 cells (79), and mouse neural stem cells (17). Therefore, the role of clathrin in JEV entry to rat neuroblastoma cells was determined using chlorpromazine, a pharmacologic inhibitor of clathrin lattice polymerization (84). Cell viability of treated B104 cells was not significantly affected by 10, 20, 30, and 40 μM chlorpromazine (Fig. 3A). To test the efficacy of chlorpromazine in clathrin endocytosis, cells were subjected to 20 μM chlorpromazine treatment and then a transferrin uptake assay was performed. As shown in Fig. 3C, a significant reduction in the signal intensity of fluorescently labeled transferrin was observed for chlorpromazine, indicating a block in transferrin uptake. The effect of chlorpromazine on JEV internalization was first assessed in the protease treatment and infectious center assay. Unexpectedly, chlorpromazine resulted in no inhibitory effect on JEV internalization (Fig. 3A). To confirm these data, B104 cells were pretreated with chlorpromazine and then inoculated with JEVpv and VSVpv. VSV, a virus that is internalized through clathrin-mediated endocytosis (30), was used as a positive control and showed significantly decreased infectivity by chlorpromazine pretreatment (Fig. 3B). However, JEVpv infection was not affected by chlorpromazine at the tested concentrations (Fig. 3B). These results suggested JEV entry to B104 cells is clathrin independent.

We next used wild-type (WT) and dominant-negative (DN) constructs of EPS 15, a required adaptor protein for clathrin-mediated endocytosis. EPS 15 directly links cargo proteins with the clathrin-coated pit adaptor protein 2 (AP-2) (5). Overexpression of the DN construct of EPS 15 selectively inhibits this process. B104 cells were transfected with plasmids expressing GFP alone,

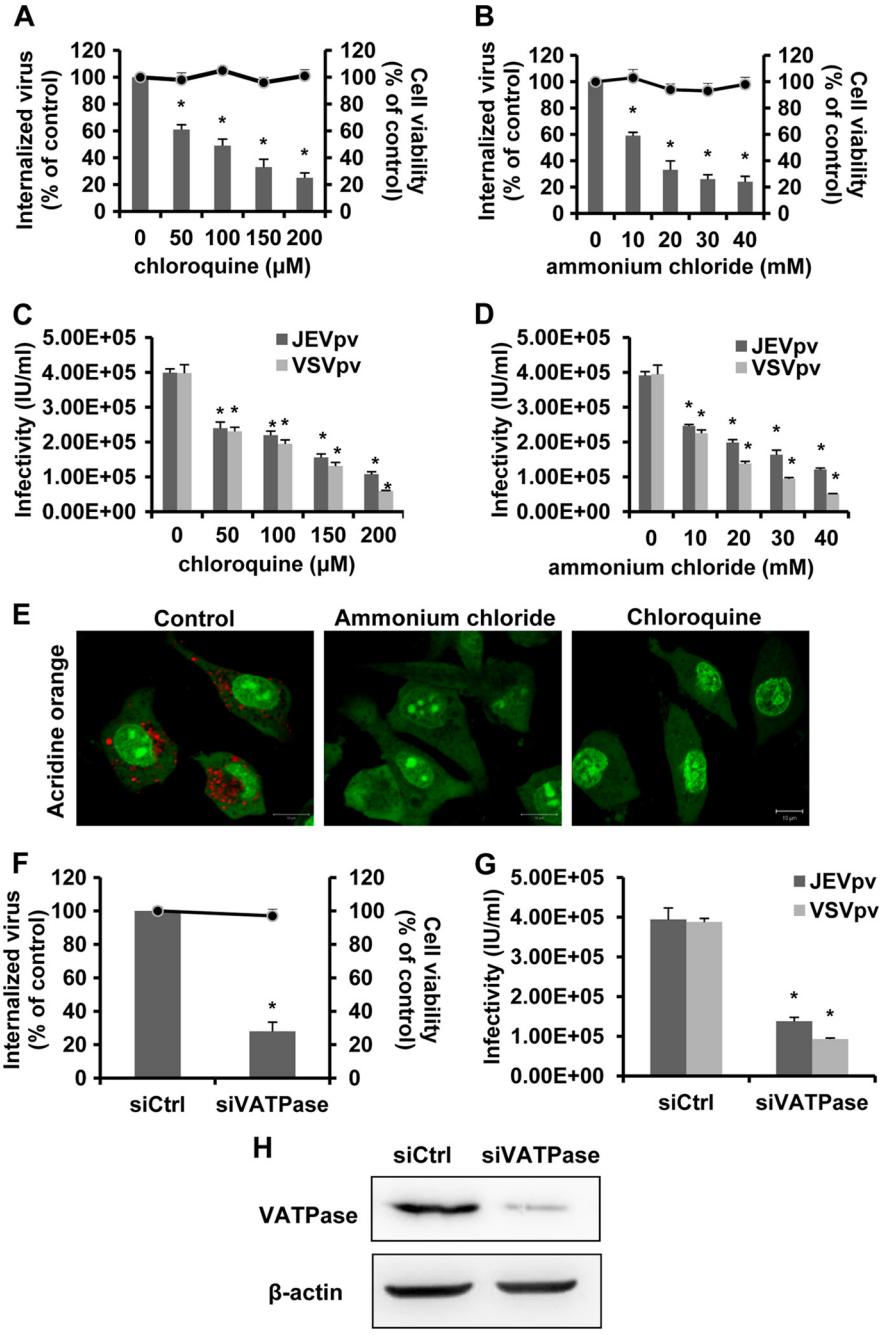

FIG 2 JEV internalization into B104 cells is dependent on acidic pH. (A and B) B104 cells were pretreated with chloroquine (A) or ammonium chloride (B) and infected with JEV. After 1 h of internalization, extracellular virus was inactivated with proteinase K and the cell pellets were plated onto B104 cells to determine internalized virus by an infectious center assay. Bar graphs represent the percentage of internalized virus with respect to a control without drug treatment. Cell viability upon drug treatments was unaffected, as represented by the line graphs. Results are presented as the means ± SD of three independent experiments. (C and D) B104 cells preincubated with chloroquine (C) or ammonium chloride (D) were inoculated with JEVpv or VSVpv. GFP-positive cells were determined by flow cytometry. Results are expressed as infectious units (IU)/milliliter and are presented as the means ± SD of three independent experiments. (E) B104 cells were left untreated (control) or treated with 100 μM chloroquine or 100 mM ammonium chloride for 1 h at 37°C. The cells then were incubated with 1 mg/ml acridine orange (AO) for 15 min, showing two distinct emission spectra: (i) green fluorescence corresponding to the monomeric AO emission, weak in the cytoplasm and bright in the nucleus; and (ii) red fluorescence from separated or aggregated compartments in the cytoplasm, corresponding to aggregated AO emission. The red fluorescence indicates an accumulation of AO in the form of dimers and/or polymers due to the acidic pH inside the compartmental lumen. Fluorescence emissions were simultaneously recorded in green (505- to 530-nm) and red (>650-nm) channels. Bars, 10 μm. (F, G, and H) B104 cells were transfected with siRNA targeting VATPase (siVATPase) or nontargeting siRNA (siCtrl) and infected with JEV (F) and JEVpv or VSVpv (G). (F) The internalized viruses (bar graphs) and cell viability (line graphs) of transfected cells were determined as in panels A and B, and the values were normalized to the value for the siCtrl. Results are presented as the means ± SD of three independent experiments. (G) GFP-positive cells were determined as in panels C and D, and the results are presented as the means ± SD of three independent experiments. (H) To verify VATPase knockdown, protein samples from cells expressing each siRNA construct were analyzed by immunoblotting for VATPase. *, $P < 0.05$.

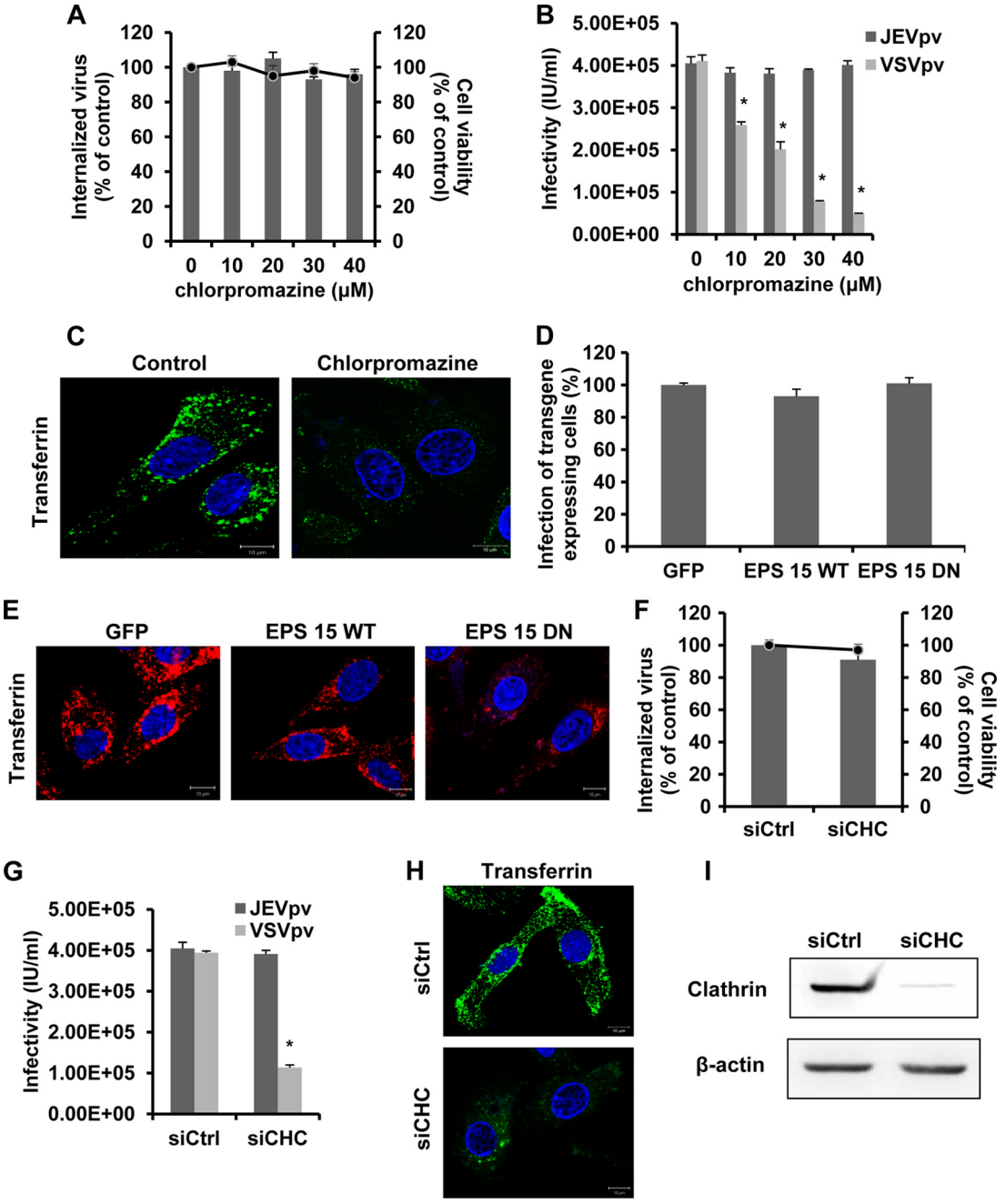

FIG 3 Clathrin is not required for JEV entry. (A) B104 cells were pretreated with chlorpromazine and infected with JEV. After 1 h of internalization, extracellular virus was inactivated with proteinase K and the cell pellets were plated onto B104 cells to determine internalized virus by an infectious center assay. Bar graphs represent the percentage of internalized virus with respect to a control without drug treatment. Cell viability upon drug treatments was unaffected, as represented by the line graphs. Results are presented as the means ± SD of three independent experiments. (B) B104 cells were pretreated with chlorpromazine and inoculated with JEVpv or VSVpv. GFP-positive cells were determined by flow cytometry. Results are expressed as infectious units (IU)/milliliter and are presented as the means ± SD of three independent experiments. (C) B104 cells were left untreated (control) or were treated with 20 μM chlorpromazine for 1 h at 37°C and then incubated with 10 μg/ml AF 488-labeled transferrin for 30 min at 37°C. Nuclei were stained with DAPI. Bars, 10 μm. (D and E) B104 cells were transfected with a GFP-only construct (GFP), the GFP-tagged wild-type construct (EPS 15 WT), or a DN EPS 15-expressing construct (EPS 15 DN) and then infected with JEV. (D) The number of JEV E-expressing cells was determined by immunofluorescence and normalized to the value for the GFP-only control. Results are presented as the means ± SD of three independent experiments. (E) B104 cells transfected with the GFP, EPS 15 WT (Dyn WT), or EPS 15 DN (Dyn DN) construct were incubated with 10 μg/ml AF 555-labeled transferrin for 30 min at 37°C. The cells then were fixed and stained with DAPI. Bars, 10 μm. (F, G, H, and I) B104 cells were transfected with the construct containing siRNA targeting clathrin heavy-chain (siCHC) or nontargeting siRNA (siCtrl) and infected with JEV (F) or JEVpv or VSVpv (G). (F) The internalized viruses (bar graphs) and cell viability (line graphs) of transfected cells were determined as in panel A, and the results were normalized to the value for the siCtrl. Results are presented as the means ± SD of three independent experiments. (G) GFP-positive cells were determined as in panel B, and the results are presented as the means ± SD of three independent experiments. (H) B104 cells transfected with siCtrl or siCHC were incubated with 10 μg/ml AF 488-labeled transferrin for 30 min at 37°C. Cells then were fixed and stained with DAPI. Bars, 10 μm. (I) To verify clathrin knockdown, protein samples from cells expressing each siRNA construct were analyzed by immunoblotting for clathrin. *, $P < 0.05$.

GFP-tagged WT EPS 15, or GFP-tagged DN EPS 15. After 48 h of transfection, cells were infected with JEV, and then the expression of E glycoprotein was measured by immunofluorescence. The number of cells expressing E protein was quantitated and normalized to the number of cells expressing GFP alone. We observed no significant change in the number of JEV E-expressing cells with the DN EPS 15 construct compared to the numbers with the WT-transfected or GFP-alone controls (Fig. 3D). The functionality of the GFP-EPS 15 constructs was verified by studying their effects on the internalization of transferrin. As expected, expression of the dominant-negative protein, but not of the control, inhibited transferrin uptake (Fig. 3E). These results further support the idea that clathrin did not play a role in JEV infection.

Furthermore, we assessed the role of clathrin during JEV entry by siRNA knockdown of clathrin heavy chain (CHC). B104 cells were transfected with a specific siRNA against CHC or a control siRNA and then infected with JEV, JEVpv, and VSVpv. No significant decrease in internalized JEV particles or JEVpv infectivity was observed in siCHC-transfected cells compared to control siRNA-transfected cells (Fig. 3F and G). In contrast, a dramatic decrease of VSVpv infectivity was observed in siCHC-transfected cells compared to siRNA control (siCtrl)-transfected cells (Fig. 3G), which is consistent with a previous study that CHC knockdown significantly reduced VSV infection (76). The effect of clathrin siRNA was assessed with AF 488-conjugated transferrin (Fig. 3H). Depletion of CHC in B104 cells was confirmed by analyzing protein samples by immunoblotting (Fig. 3I). Consequently, it is valid to conclude that JEV entry into rat neuroblastoma cells is independent of clathrin.

JEV endocytosis to rat neuroblastoma cells depends on dynamin. Dynamin is a GTPase essential for pinching off endosomes from the cytoplasma membrane (39). Since dynamin II has been shown to be required for the internalization of numerous viruses, we analyzed its role in JEV entry. For this, we obtained dynasore, a cell-permeable, noncompetitive dynamin GTPase activity inhibitor (36). B104 cells were pretreated with dynasore and infected with JEV, JEVpv, and VSVpv. Minimal cellular cytotoxicity was observed in dynasore-treated cells (Fig. 4A). JEV internalization was significantly inhibited by dynasore pretreatment in a dose-dependent manner (Fig. 4A). Similarly, more than 70% inhibition of JEVpv infectivity at 160 μM dynasore was observed (Fig. 4B). As a control, dynasore effectively blocked the VSV entry (Fig. 4B), which requires dynamin II for its uptake via clathrin-mediated endocytosis (76). A significant reduction in the signal intensity of fluorescently labeled transferrin was observed for dynasore-treated cells compared to untreated cells (Fig. 4C), indicating a block in transferrin uptake. The results with dynasore suggest that dynamin is needed for JEV endocytosis.

To further determine the role of dynamin during JEV entry, the effect of the dynamin II DN construct on viral antigen expression was tested. B104 cells were transfected with WT and DN constructs prior to infection, and virus-infected cells were quantitated by staining for JEV E protein. The expression of DN dynamin II K44A mutant resulted in approximately 75% inhibition of the number of JEV E-expressing cells, compared to the corresponding WT construct (Fig. 4D). The functionality of the dynamin II constructs was proved by an assay of the transfer of incorporation in transfected cells. As expected, expression of the dominant-negative protein, but not of the control, inhibited transferrin uptake (Fig. 4E). These results demonstrate that JEV infection requires dynamin II.

To confirm the findings above, we silenced dynamin II expression by siRNA treatment. B104 cells were transfected with a specific siRNA against dynamin II or a control siRNA, and then infected with JEV, JEVpv, and VSVpv. Depletion of dynamin II led to a significant decrease in JEV internalization and entry (Fig. 4F and G). Dynamin II siRNA did not cause obvious cell death (Fig. 4F). The effectiveness of dynamin II depletion in B104 cells was controlled by Western blotting (Fig. 4H). The effect of dynamin II siRNA was assessed with AF 488-conjugated transferrin (Fig. 4I). Together, these data demonstrate that JEV entry occurs through a dynamin-dependent endocytosis.

JEV enters rat neuroblastoma cells via a caveola-mediated endocytosis pathway. Dynamin was originally considered to participate in clathrin-dependent endocytosis only but has recently been implicated in several other endocytic pathways (18). Another form of endocytosis that requires dynamin is caveola-mediated uptake. Membrane cholesterol is a prominent component of lipid rafts and is required for formation of caveolae. Depletion of cholesterol from the membrane with methyl-β-cyclodextrin (MβCD) or sequestration of cholesterol with filipin has been shown to impair caveola-mediated endocytosis (61, 67). The effects of MβCD or filipin on JEV entry were determined by viral internalization and pseudoparticle infection assays. When B104 cells were pretreated with increasing concentrations of filipin prior to infection, JEV entry was inhibited in a dose-dependent manner (Fig. 5A and B). Consistent with the results obtained with filipin, infection by JEV and JEVpv was significantly inhibited in cells pretreated with MβCD (Fig. 5C and D). More than 75% inhibition at 10 mM MβCD can be observed. Since high concentrations of MβCD not only inhibit cholesterol-dependent mechanisms but can also affect clathrin-mediated endocytosis (82), we assessed the effect of 10 mM MβCD on VSV endocytosis. As shown in Fig. 5D, pretreatment of 10 mM MβCD did not reduce entry of VSV, a virus that uses cholesterol-independent clathrin-mediated endocytosis to infect cells (76). In order to determine whether MβCD treatment depletes cellular cholesterol levels, we quantitated the amounts of cellular cholesterol before and after MβCD treatment. The total intracellular pools of cholesterol were reduced by 60% in 10 mM MβCD-treated B104 cells compared to those of untreated cells (Fig. 5E). Cholera toxin B (CTB) enters cells by binding to its receptor gangliosides (GM1) in a caveola-dependent manner, which shows a characteristic perinuclear vesicular accumulation (22, 38). The internalization of fluorescently labeled CTB was shown to determine the effectiveness of MBCD and filipin. As shown in Fig. 5F, untreated cells allowed CTB uptake and showed a clear, dotted perinuclear cytoplasmic fluorescence, whereas cells treated with MBCD or filipin were impaired in internalization of CTB. These observations suggested that JEV entry was associated with the levels of membrane cholesterol.

Internalization of caveolae depends on specific signaling events (73), including activation of protein kinase C (43) and tyrosine phosphorylation (51, 57). Here, we tested the effects of genistein and okadaic acid on JEV entry. B104 cells were first pretreated with increasing concentrations of genistein, a specific tyrosine kinase inhibitor, and then infected with JEV or JEVpv. As shown in Fig. 6A, treatment of cells with 10, 50, 100, and 200 μM genistein inhibited JEV internalization by approximately 12, 25, 39, and 64%, respectively, compared to that of the untreated control. Ge-

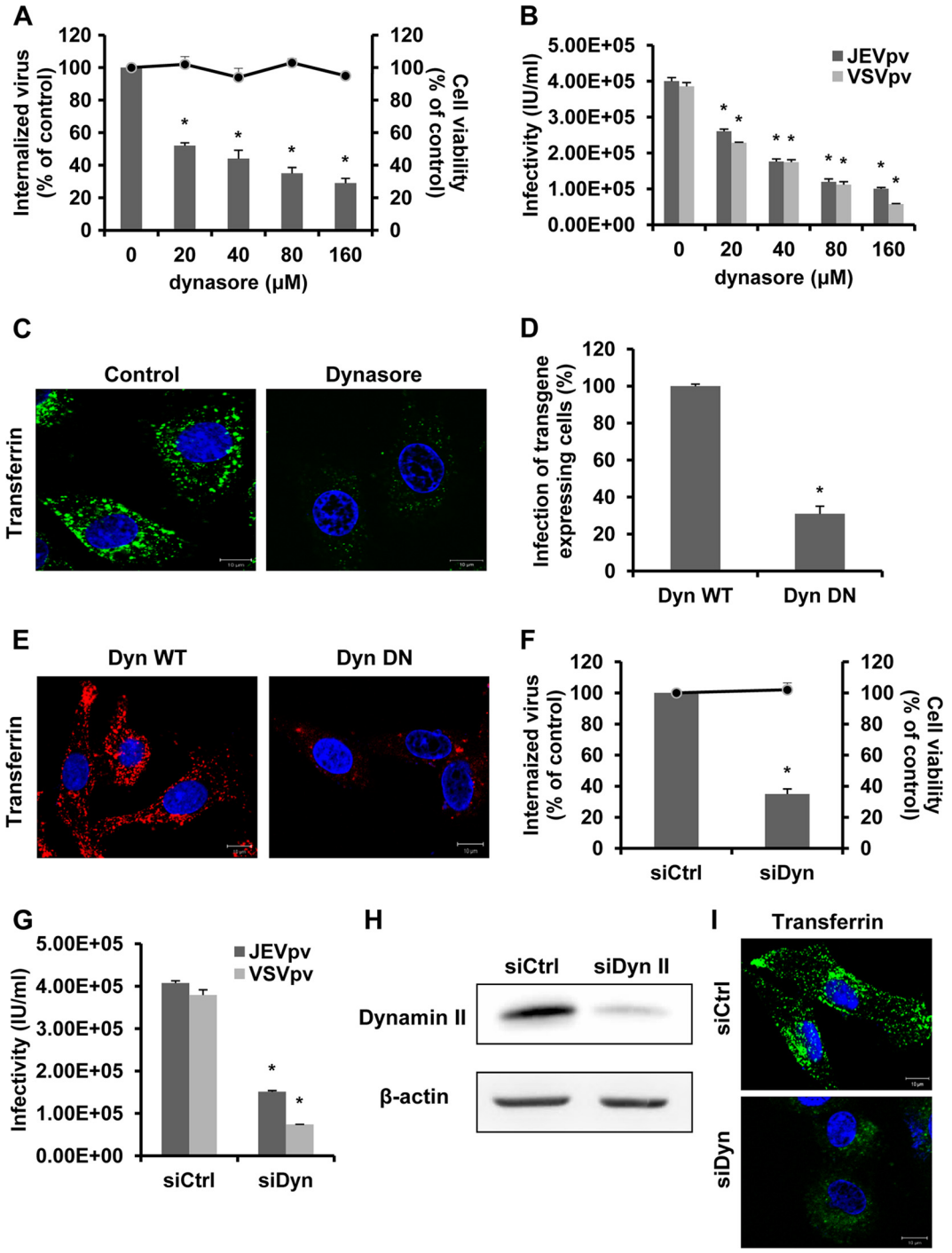

FIG 4 JEV entry depends on dynamin II. (A) B104 cells were pretreated with dynasore and infected with JEV. After 1 h of internalization, extracellular virus was inactivated with proteinase K and the cell pellets were plated onto B104 cells to determine internalized virus by an infectious center assay. Bar graphs represent the percentage of internalized virus with respect to a control without drug treatment. Cell viability upon drug treatments was unaffected, as represented by the line graphs. Results are presented as the means ± SD of three independent experiments. (B) B104 cells were pretreated with dynasore and inoculated with JEVpv or VSVpv. GFP-positive cells were determined by flow cytometry. Results are expressed as infectious units (IU)/milliliter and are presented as the means ± SD of three independent experiments. (C) B104 cells were left untreated (control) or treated with 40 μM dynasore for 1 h at 37°C and then incubated with 10 μg/ml AF 488-labeled transferrin for 30 min at 37°C. Nuclei were stained with DAPI. Bars, 10 μm. (D and E) B104 cells were transfected with the GFP-tagged WT dynamin (Dyn WT) or DN construct (Dyn DN) and then infected with JEV. (D) The number of JEV E-expressing cells was determined by immunofluorescence and normalized to the value for the Dyn WT. Results are presented as the means ± SD of three independent experiments. (E) B104 cells transfected with Dyn WT or Dyn DN were incubated with 10 μg/ml AF 555-labeled transferrin for 30 min at 37°C. The cells then were fixed and stained with DAPI. Bars, 10 μm. (F, G, H, and I) B104 cells were transfected with the construct containing siRNA targeting dynamin II (siDyn) or the nontargeting siRNA (siCtrl) and infected with JEV (F) or JEVpv or VSVpv (G). (F) The internalized viruses (bar graphs) and cell viability (line graphs) of transfected cells were determined as in panel A and normalized to the value for the siCtrl. Results are presented as the means ± SD of three independent experiments. (G) GFP-positive cells were determined as in panel B, and the results are presented as the means ± SD of three independent experiments. (H) To verify dynamin II knockdown, protein samples from cells expressing each siRNA construct were analyzed by immunoblotting for dynamin II. (I) B104 cells transfected with siCtrl or siDyn were incubated with 10 μg/ml AF 488-labeled transferrin for 30 min at 37°C. The cells then were fixed and stained with DAPI. Bars, 10 μm. *, $P < 0.05$.

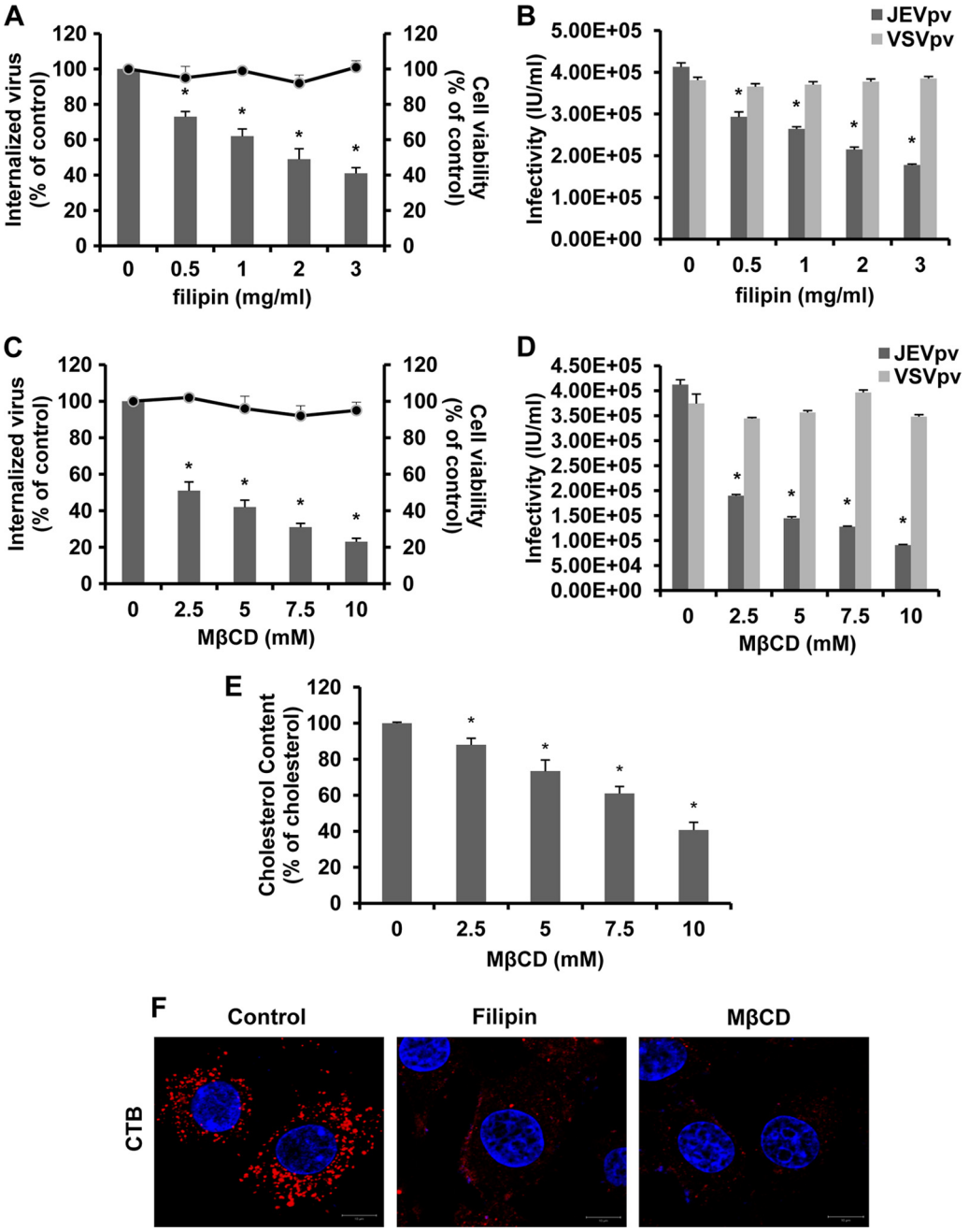

FIG 5 Filipin and MβCD inhibit JEV entry into B104 cells. (A and C) B104 cells were pretreated with filipin (A) or MβCD (C) and infected with JEV. After 1 h of internalization, extracellular virus was inactivated with proteinase K and the cell pellets were plated onto B104 cells to determine internalized virus by an infectious center assay. Bar graphs represent the percentage of internalized virus with respect to a control without drug treatment. Cell viability upon drug treatments was unaffected, as represented by the line graphs. Results are presented as the means ± SD of three independent experiments. (B and D) B104 cells preincubated with filipin (B) or MβCD (D) were inoculated with JEVpv or VSVpv. GFP-positive cells were determined by flow cytometry. Results are expressed as infectious units (IU)/milliliter and are presented as the means ± SD of three independent experiments. (E) Intracellular cholesterol levels were quantitated in mock-treated or MβCD-treated B104 cells and compared to those in mock-treated B104 cells. Results are expressed as the means ± SD of three independent experiments. (F) B104 cells were left untreated (control) or were treated with 1 mg/ml filipin or 10 mM MβCD for 1 h at 37°C and then incubated with 10 μg/ml AF 555-labeled cholera toxin B (CTB) for 30 min at 37°C. Nuclei were stained with DAPI. Bars, 10 μm. *, $P < 0.05$.

nistein also inhibited JEVpv infection in a dose-dependent manner (Fig. 6B). Moreover, cells were pretreated with okadaic acid, a general inhibitor of serine and threonine phosphatases that is known to increase caveolar endocytosis and to inhibit the clathrin-mediated entry pathway (54, 81). As shown in Fig. 6C, treatments with 0.1 and 0.2 μM okadaic acid had no effect on JEV internalization, while 0.5 to 1 μM okadaic acid significantly enhanced the uptake of JEV. Similarly, treatment of B104 cells with okadaic acid increased the infectivity of JEVpv (Fig. 6D). As expected, VSVpv infection was inhibited by okadaic acid (Fig. 6D).

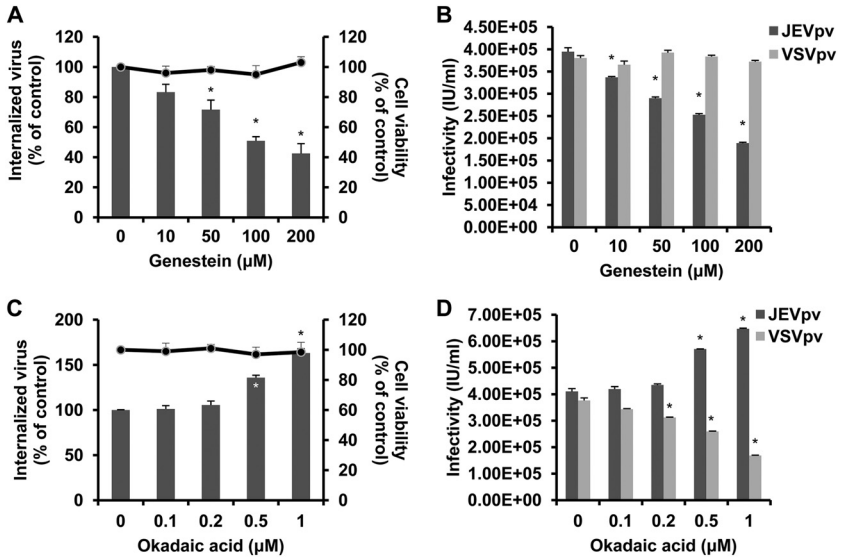

FIG 6 Effects of genistein and okadaic acid on JEV entry. (A and C) B104 cells were pretreated with genistein (A) or okadaic acid (C) and infected with JEV. After 1 h of internalization, extracellular virus was inactivated with proteinase K and the cell pellets were plated onto B104 cells to determine internalized virus by an infectious center assay. Bar graphs represent the percentage of internalized virus with respect to that of a control without drug treatment. Cell viability upon drug treatments was unaffected, as represented by the line graphs. Results are presented as the means ± SD of three independent experiments. (B and D) B104 cells preincubated with genistein (B) or okadaic acid (D) were inoculated with JEVpv or VSVpv. GFP-positive cells were determined by flow cytometry. Results are expressed as infectious units (IU)/milliliter and are presented as the means ± SD of three independent experiments. *, $P < 0.05$.

These results suggest JEV-induced transmembrane signaling is important for efficient virus entry into host cells.

Caveolins are essential for the formation and stability of caveolae. In the absence of caveolins, no caveolae are observed, and when caveolins are expressed in cells that lack caveolae, they induce caveola formation (21). To block caveola-mediated endocytosis, we expressed a previously characterized DN caveolin-1 (DN Cav) in B104 cells (14). Cells transfected with the DN Cav or WT Cav constructs were infected by JEV and then subjected to immunofluorescence. As shown in Fig. 7A, a significant decrease in the number of JEV E-expressing cells was observed in cells transfected with DN Cav compared to the WT Cav-transfected cells, suggesting the involvement of caveolin-1 in JEV infection. These results were confirmed by siRNA knockdown of caveolin-1. B104 cells were transfected with siRNA targeting caveolin-1 (siCav-1) or a control siRNA and then infected with JEV and JEVpv. Treatment of siCav-1 significantly reduced JEV internalization and entry into B104 cells compared to the control siRNA treatment (Fig. 7B and C). The silencing efficiency of the siCav-1 was analyzed by Western blotting (Fig. 7D). These data strongly suggest the involvement of caveolin-1 for internalization of JEV virions.

We next examined the internalization of JEV and specific endocytic markers by B104 cells. JEV (MOI, 1) and 10 μg/ml AF 555-conjugated CTB or AF 555-conjugated transferrin were permitted to bind to cells at 4°C for 30 min. The cells then were shifted to 37°C for 1 h to allow internalization, washed extensively, fixed, and analyzed by immunofluorescence microscopy using anti-JEV E antibodies. As shown in Fig. 8A, both JEV and CTB showed characteristic perinuclear staining, and colocalization of virus with CTB was also observed within this region. However, the clathrin-dependent endocytosis marker, transferrin, did not appear to overlap JEV inside the cell (Fig. 8B).

To further demonstrate that JEV entry is mediated by caveolae,

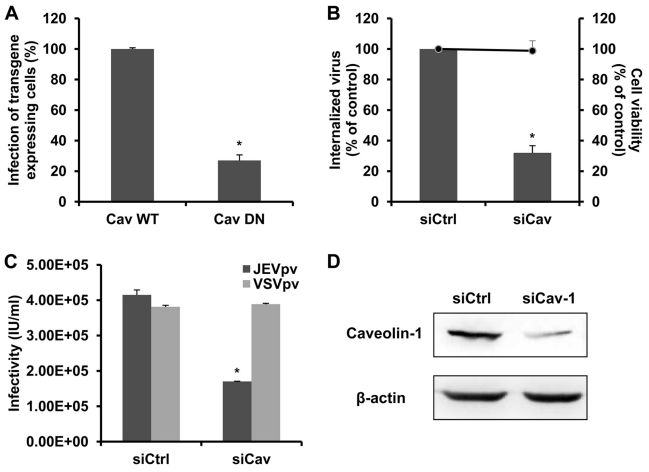

FIG 7 Dominant-negative construct and siRNA targeting caveolin-1 inhibit JEV internalization. (A) B104 cells were transfected with a GFP-tagged WT caveolin-1 construct (Cav WT) or caveolin-1 DN construct (Cav DN) and then infected with JEV. The number of JEV E-expressing cells was determined by immunofluorescence and normalized to the value for the Cav WT. Results are presented as the means ± SD of three independent experiments. (B, C, and D) B104 cells were transfected with a construct containing siRNA targeting caveolin-1 (siCav) or nontargeting siRNA (siCtrl) and infected with JEV (B) or JEVpv or VSVpv (C). (B) The internalized viruses (bar graphs) and cell viability (line graphs) of transfected cells were determined as described in Materials and Methods and normalized to the value for the siCtrl. Results are presented as the means ± SD of three independent experiments. (C) GFP-positive cells were determined as in Materials and Methods and are presented as the means ± SD of three independent experiments. (D) To verify caveolin-1 knockdown, protein samples from cells expressing each siRNA construct were analyzed by immunoblotting for caveolin-1. *, $P < 0.05$.

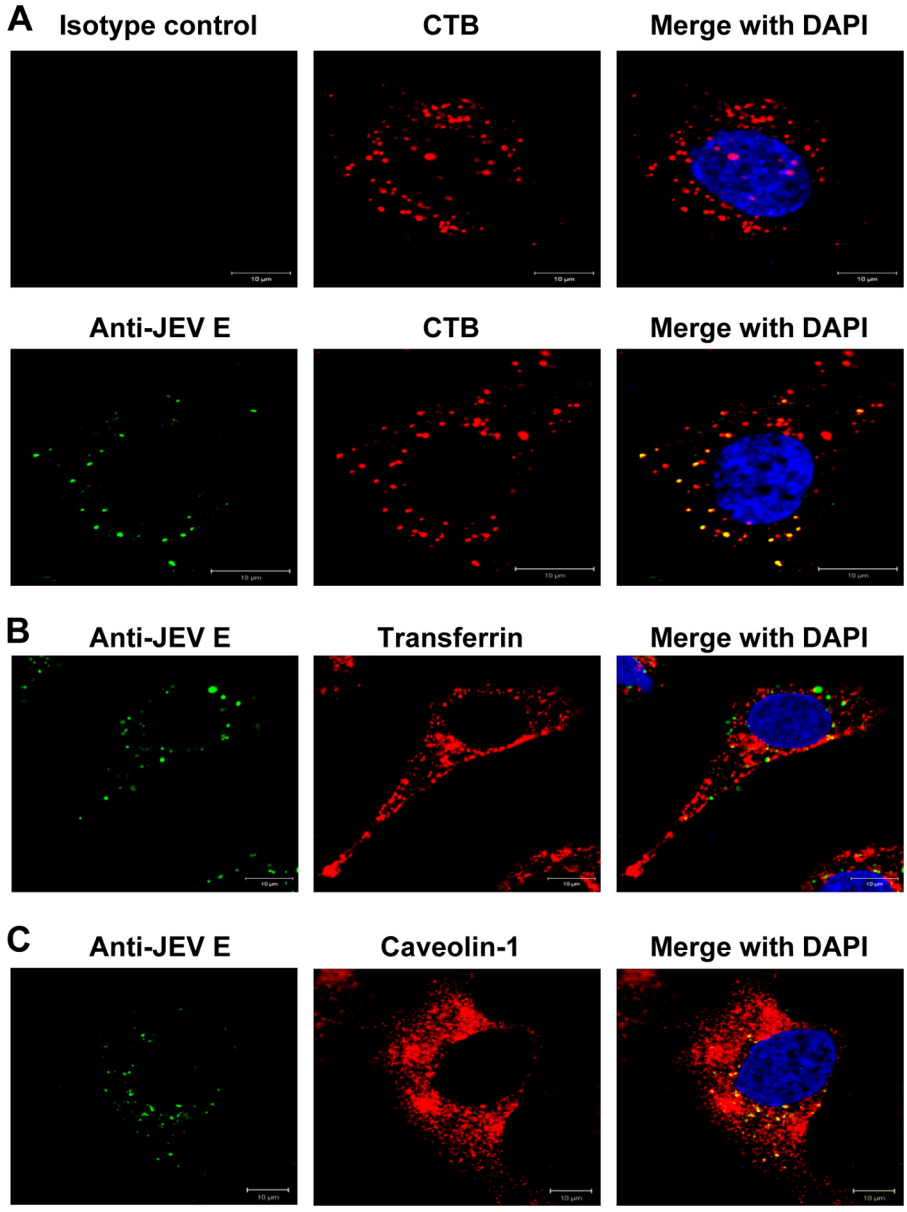

FIG 8 Colocalization of JEV with endocytic markers. (A and B) B104 cells seeded on coverslips were washed twice with PBS and incubated for 30 min at 4°C with JEV (MOI, 1) and 10 μg/ml AF 555-conjugated CTB (A) or 10 μg/ml AF 555-conjugated transferrin (B). After attachment at 4°C, cells were transferred to 37°C for 1 h to allow the endocytosis of JEV, CTB, and transferrin. Cells were washed twice with PBS and then analyzed by immunofluorescence staining using anti-JEV E mouse monoclonal antibody (A, lower panels) or an isotype control (A, upper panels) and AF 488-labeled goat anti-mouse IgG. Nuclei were stained with DAPI. (C) Virus attachment was permitted as in panels A and B, and virus internalization was allowed at 37°C for 1 h. Cells were then washed, fixed, and stained with anti-JEV E antibody and anti-caveolin-1 antibody, followed by fluorescent-labeled secondary antibodies. Nuclei were counterstained with DAPI. Bars, 10 μm.

cells were incubated with JEV at 4°C to allow virus attachment and then shifted to 37°C for 1 h to allow internalization, after which the cells were subjected to fixation and immunofluorescence staining with antibodies specific for JEV E and caveolin-1. As shown in Fig. 8C, most of the internalized JEV particles colocalized with caveolin-1. Altogether, we can conclude that the infectious entry of JEV into rat neuroblastoma cells is dependent on caveola-mediated endocytosis.

JEV entry into rat neuroblastoma cells is independent of macropinocytosis/phagocytosis. Dynamin II and cholesterol can play a role in macropinocytosis and phagocytosis (69). Although neither macropinocytosis nor phagocytosis is frequently involved in flavivirus entry, they have been reported as an alternative means of access for some viruses in certain cells (3, 13, 37). To address the importance of macropinocytosis/phagocytosis as an entry mechanism for JEV, we examined the effect of 5-ethyl-*N*-isopropyl amiloride (EIPA), an inhibitor of macropinocytosis that blocks Na^+/H^+ exchange (85), on JEV internalization and JEVpv infection. Pretreatment of B104 cells with EIPA did not lead to a decrease in JEV entry (Fig. 9A and B). Cell viability of treated cells was unaffected by EIPA at the concentrations used in these experiments (Fig. 9A). Dextran was used to monitor the effect of EIPA.

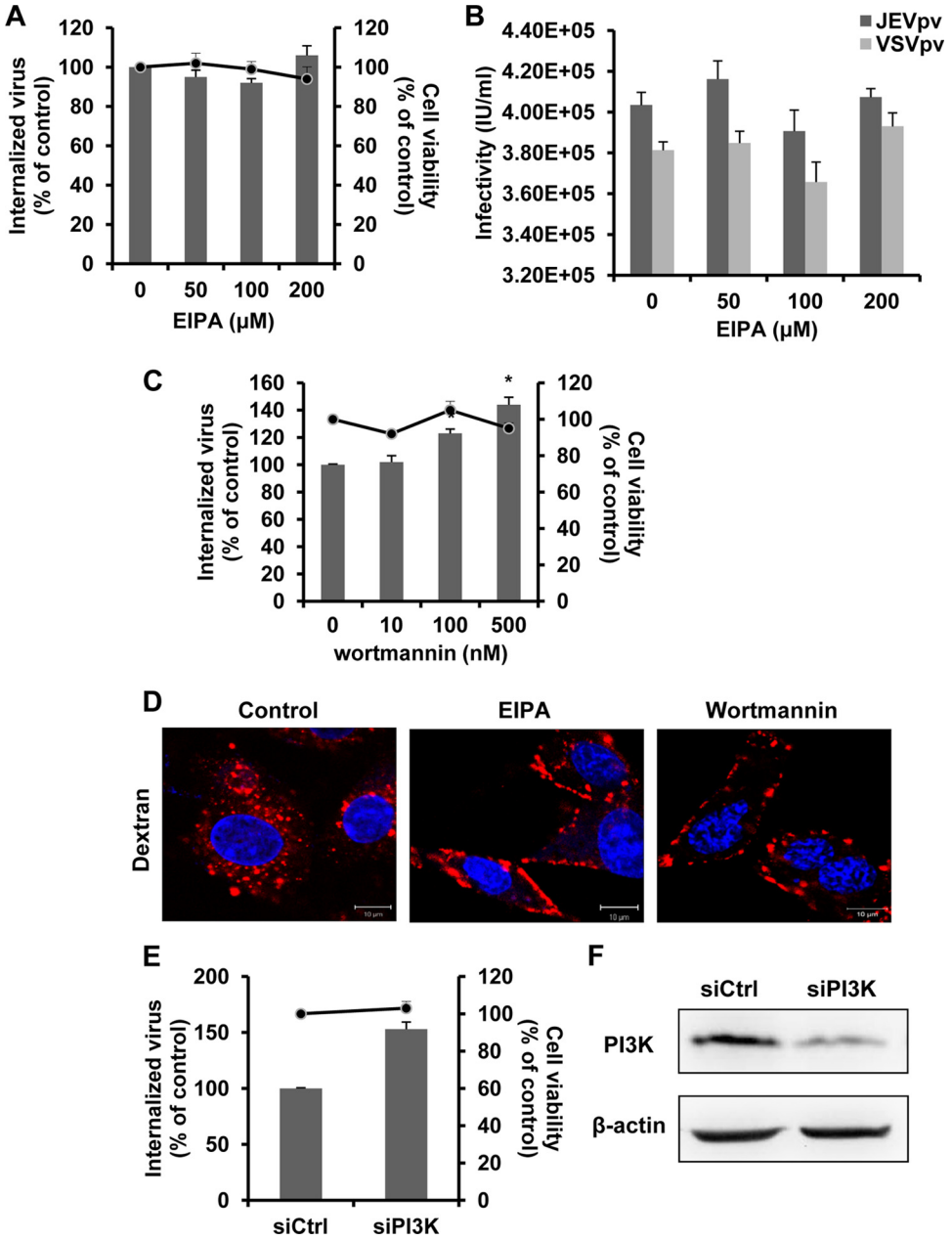

FIG 9 JEV entry is independent of macropinocytosis/phagocytosis. (A and C) B104 cells were pretreated with EIPA (A) or wortmannin (C) and infected with JEV. After 1 h of internalization, extracellular virus was inactivated with proteinase K and the cell pellets were plated onto B104 cells to determine internalized virus by an infectious center assay. Bar graphs represent the percentage of internalized virus with respect to a control without drug treatment. Cell viability upon drug treatments was unaffected, as represented by the line graphs. Results are presented as the means ± SD of three independent experiments. (B) B104 cells preincubated with EIPA were inoculated with JEVpv or VSVpv. GFP-positive cells were determined by flow cytometry. Results are expressed as infectious units (IU)/milliliter and presented as the means ± SD of three independent experiments. (D) B104 cells were left untreated (control) or were treated with 50 μM EIPA or 50 nM wortmannin for 1 h at 37°C and then incubated with 200 μg/ml AF 555-conjugated dextran for 30 min at 37°C. Nuclei were stained with DAPI. Bars, 10 μm. (E and F) B104 cells were transfected with the construct containing siRNA targeting PI3K (siPI3K) or nontargeting siRNA (siCtrl) and infected with JEV. (E) The internalized viruses (bar graphs) and cell viability (line graphs) of transfected cells were determined as in panel A and normalized to the value for the siCtrl. Results are presented as the means ± SD of three independent experiments. (F) To verify PI3K knockdown, protein samples from cells expressing each siRNA construct were analyzed by immunoblotting for PI3K. *, $P < 0.05$.

As expected, EIPA totally blocked the internalization of dextran (Fig. 9D). These results suggest minimal involvement of macropinocytosis/phagocytosis in JEV entry.

During the process of macropinocytosis/phagocytosis, a number of cell-type-dependent factors can be required—e.g., phosphatidylinositol 3-kinase (PI3K), Rac1, and Cdc42. To validate the findings presented above, we utilized wortmannin, an inhibitor of PI3K (35). As shown in Fig. 9C, no inhibition was observed on JEV entry after treatment with the PI3K inhibitor. Wortmannin effectively blocked the internalization of dextran (Fig. 9D).

Consistent with the results obtained with wortmannin, JEV internalization was not inhibited in B104 cells transfected with siRNA against PI3K; instead, depletion of this macropinocytosis regulatory molecule seemed to enhance JEV entry (Fig. 9E). Efficiency of siRNA-mediated knockdown of PI3K was controlled by immunoblotting (Fig. 9F). In a word, our results suggest that the endocytosis of JEV to rat neuroblastoma cells is not dependent on macropinocytosis/phagocytosis.

JEV entry does not use clathrin-mediated endocytosis and macropinocytosis/phagocytosis as a minor route of productive infection. Overall, our data demonstrate a role for both dynamin and cholesterol or caveolin-1 during JEV entry. However, no pharmacologic treatment, expression of DN constructs, or siRNA treatment was able to decrease JEV entry or infection below 20%. This suggested that none of these inhibitors, DN constructs, or siRNAs can fully inhibit these processes or that the virus can productively enter the cell by more than one pathway. Many viruses are known to enter cells via multiple routes, such as echovirus 1 (EV1) (caveola- and dynamin-2-dependent pathways) (38), influenza virus (both clathrin-dependent and clathrin-independent routes) (52, 70), and DENV (clathrin-mediated endocytosis and macropinocytosis) (75). To test the hypothesis that JEV enters B104 cells by more than one productive pathway, we tested combinations of inhibitors in the proteinase K assay. B104 cells were pretreated with combinations of 2.5 mM MβCD and other inhibitors (chloroquine, chlorpromazine, dynasore, EIPA, and wortmannin) prior to JEV infection, and then the proteinase K infectious assay was performed as described above. Combination treatment of chlorpromazine and MβCD did not significantly reduce viral entry compared to MβCD-only treatment (Fig. 10A), suggesting that clathrin-mediated endocytosis did not play a role in JEV infection. Further decrease of viral entry was observed by addition of dynasore and MβCD or chloroquine and MβCD compared to addition of MβCD alone (Fig. 10A). In addition, the combination of dynasore, chloroquine, and MβCD treatment almost inhibited JEV internalization completely, suggesting the requirement of dynamin, caveolae, and an acidic environment for JEV entry into B104 cells (Fig. 10A). Interestingly, a significant increase in viral entry was observed in MβCD- and EIPA- or wortmannin-treated cells (Fig. 10A). The infectivity data of JEVpv confirmed that clathrin-mediated endocytosis and phagocytosis/macropinocytosis did not play minor roles during JEV entry into rat neuroblastoma cells (Fig. 10B).

The endocytotic pathways utilized by JEV to enter rat neuroblastoma cells are not virus strain specific. To determine whether other JEV strains also use a clathrin-independent, caveola-dependent internalization route, using the infectious center assay we assessed the effect of the pharmacological inhibitors on the internalization of the wild-type virus SA14 belonging to genotype III (GenBank accession no. U14163.1) and an isolated JEV strain, SH-53, belonging to genotype I (GenBank accession no. AY55574). As shown in Fig. 11, no inhibitory effect on the internalization of JEV strain SA14 and SH-53 was detected by chlorpromazine or EIPA treatment. However, MβCD, chloroquine, and dynasore all resulted in a significant reduction in the internalization of different JEV genotypes (Fig. 11). These results suggest that the atypical dynamin-dependent caveola-mediated pathway for JEV entry into B104 cells is virus strain independent.

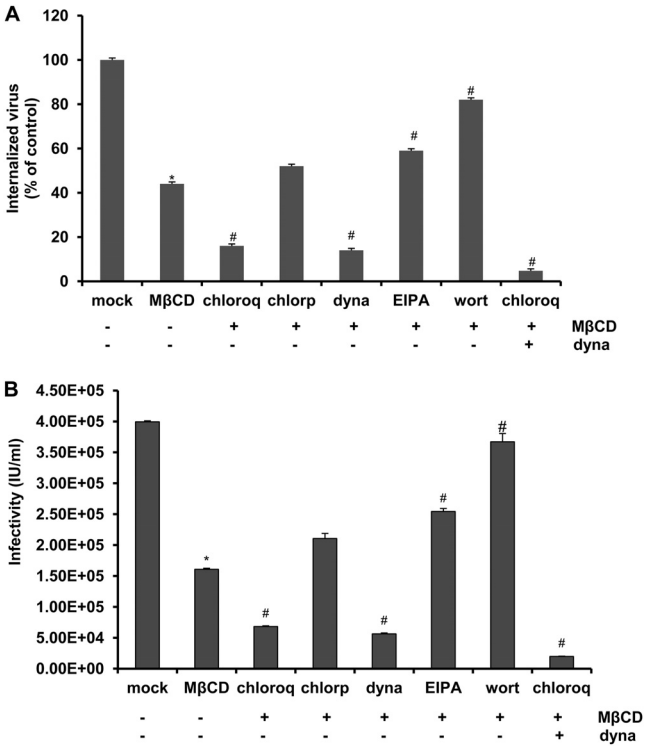

FIG 10 Clathrin-dependent endocytosis or phagocytosis/macropinocytosis is not a minor route of entry for JEV. B104 cells were pretreated for 1 h at 37°C with 2.5 mM MβCD alone (−), 2.5 mM MβCD and 50 μM chloroquine (chloroq), 2.5 mM MβCD and 40 μM chlorpromazine (chlorp), 2.5 mM MβCD and 40 μM dynasore (dyna), 2.5 mM MβCD and 100 μM amiloride (EIPA), 2.5 mM MβCD and 100 μM wortmanin (wort), or the combination of 2.5 mM MβCD, 50 μM chloroquine (chloroq), and 40 μM dynasore (dyna). The cells then were infected with JEV (A) or JEVpv (B) for 1 h at 37°C. (A) After 1 h of internalization, extracellular virus was inactivated with proteinase K and the cell pellets were plated onto B104 cells to determine internalized virus by an infectious center assay. Bar graphs with * represent the percentage of internalized virus with respect to a mock control. Bar graphs with # represent the percentage of internalized virus with respect to a control with 2.5 mM MβCD alone (−). Results are expressed as the means ± SD of three independent experiments. (B) GFP-positive cells were determined by flow cytometry. Bar graphs with * represent the infectious units (IU)/milliliter with respect to a mock control. Bar graphs with # represent the IU/milliliter with respect to a control with 2.5 mM MβCD alone (−). Results are expressed as the means ± SD of three independent experiments. *, $P < 0.05$; #, $P < 0.05$.

DISCUSSION

Many viruses require the cellular mechanism of endocytosis to mediate their infectious entry into host cells. In this study, the data demonstrate that JEV uptake occurs within 1 h and that the infectious entry pathway of JEV into rat neuroblastoma cells requires both caveolae and dynamin. We also showed that JEV entry to B104 cells is neither clathrin nor macropinocytosis/phagocytosis dependent but involves endosomal acidification.

The internalization of flaviviruses was considered at acid pH, and the low-pH environment within endosomes triggers a series of molecular events of the flavivirus E glycoprotein leading to membrane fusion of the viral membrane with the endosomal membrane and subsequent release of the nucleocapsid into the cell cytosol (28). Our results showed that JEV cell entry is sensitive to elevation of the pH in intracellular acidic compartments, as suggested by Tani et al. (79). Traditionally, viral entry through

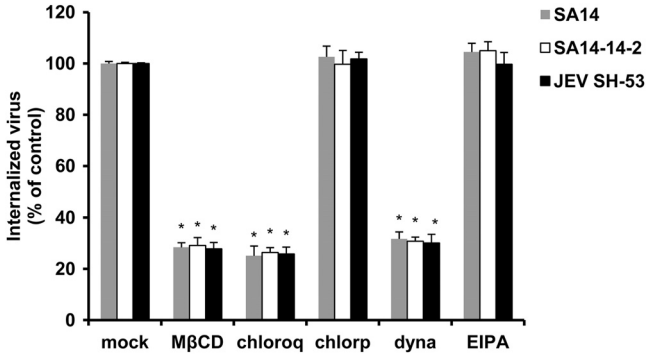

FIG 11 The endocytotic pathways utilized by JEV are virus strain independent. B104 cells were pretreated for 1 h at 37°C with 10 mM MβCD, 200 μM chloroquine (chloroq), 40 μM chlorpromazine (chlorp), 160 μM dynasore (dyna), or 200 μM amiloride (EIPA). Cells were then infected with JEV wild-type virus SA14, JEV attenuated strain SA14-14-2, or an isolated JEV strain, SH-53, separately. After 1 h of internalization, extracellular virus was inactivated with proteinase K and the cell pellets were plated onto B104 cells to determine internalized virus by an infectious center assay. Bar graphs represent the percentage of internalized virus with respect to a control without drug treatment. Results are presented as the means ± SD of three independent experiments. *, $P < 0.05$.

caveolae is considered to occur in a pH-neutral setting, bypassing the acidic endosomal route (4, 59). Besides the classical caveola-caveosome-endoplasmic reticulum uptake, a nonclassical endosomal structure that tests positive for calveolin-1 has been shown to deliver caveola-internalized cargo to the Golgi complex, an organelle with an acidic pH ranging from 6.0 to 6.7 (33). Although few flaviviruses are reported to enter cells in this manner, an increasing number of enveloped viruses use a pH-dependent, cholesterol-dependent, and caveolin-1-sensitive endocytosis via caveolae, including Newcastle disease virus (7), tiger frog virus (27), BK virus (19), Ebola virus, and Marburg virus (66).

Dynamin is a high-molecular-weight GTPase involved in the scission of nascent vesicles from parent membranes during endocytic events. It has been reported that dynamin is a central regulator of several types of endocytosis and is needed for the internalization of numerous viruses (27, 60, 62). However, little is currently known about the participation of dynamin in the entry process of JEV. In the present study, the essential role of dynamin in the endocytosis of JEV was suggested. Although dynamin activity was initially thought to be specific to clathrin-mediated endocytosis (15), our data imply that dynamin plays an important role in JEV cell entry through caveola-mediated endocytosis but independent of clathrin. It appears to form a structural collar around the neck of caveolae that hydrolyzes GTP to mediate internalization via the fission of caveolae from the plasma membrane to form free transport vesicles (53).

We investigated the role of alternative or minor routes of JEV entry by treatments with combinations of inhibitors. Treatment with MβCD and dynasore together showed a significant decrease in the amount of JEV entry over MβCD treatment alone, raising another possibility that the two compounds block two independent pathways, and, therefore, a larger reduction in internalized virus is seen. If one pathway is blocked, a small percentage of virions may enter through an alternative route; but if the alternative route is also inhibited, the overall capacity of the virus to infect the cell is further reduced. Interestingly, wortmannin significantly increased the amount of JEV entry. The enhancement of viral infectivity was observed even in the presence of both MβCD and wortmannin. The possible explanation given here is that the phagocytosis/macropinocytosis pathway would be a noninfective route of entry for JEV in B104 cells, and, consequently, when it is blocked, there is an enhancement in the utilization by JEV virions of the infective nonphagocytosis/macropinocytosis pathway, leading to higher production of infectious virus.

To compare the routes of entry of JEV in other types of mammalian cells different from B104, the viral internalization of Vero and CHO cells in the presence of pharmacological inhibitors of endocytosis and specific siRNA for clathrin or caveolin-1 was also assayed. The results showed that except for B104 cells, entry of JEV into the other cell lines was dependent on clathrin but independent of caveolin (data not shown), which was consistent with the previous studies (49). At present, the mechanistic basis of the differences in clathrin dependence for JEV entry to diverse host cells cannot be fully understood. The type of pathways exploited may be explained in terms of the use of different virus receptors (71). The interactions between virus particles and their receptors at the cell surface determine the mechanisms of virus attachment, uptake, intracellular trafficking, and, ultimately, penetration to the cytosol. Although the exact receptor(s) on B104 cells is unknown, a number of cellular components, such as $\alpha_v\beta_3$ integrin in Vero cells (11) and low-density lipoprotein receptor (LDLR) in CHO cells (9), have been shown to be involved in JEV infection. According to recent data, Sancey et al. found $\alpha_v\beta_3$ integrin to be rapidly internalized in clathrin-coated pits, thus, enhancing the uptake of arginine-glycine-aspartic acid (RGD)-containing peptides (65). Similarly, LDLR had been earlier found to undergo endocytosis by a clathrin-dependent mechanism (23). Therefore, it is possible to hypothesize that the receptor(s) used by JEV for entry into B104 cells may be localized in or recruited to caveolae, thus initiating the caveola-mediated endocytosis.

Why are caveolae, but not clathrin, used as an entry port for neuroblastoma cells by JEV? It was recently demonstrated that endocytic transport and signal transduction are tightly coupled (58). In general, signaling during endocytosis is compartmentalized (74). This compartmentalization of signaling provides for a variety of cellular effects that viruses may take advantage of by choosing a particular endocytic pathway (69). Although JEV can infect and replicate in a wide range of cells of different origins *in vitro*, it is neurotropic *in vivo*. Is the caveola-mediated endocytosis relevant for JEV's neurotropism? It is known that JEV causes neuronal cell death in two ways—direct neuronal killing (63), wherein viral multiplication within neuronal cells leads to cell apoptosis or necrosis, and the indirect mode of killing (25), wherein a massive inflammatory response causes upregulation of reactive oxygen species and cytokines, which in turn causes neuronal death. Both direct and indirect ways are mediated by specific kinases and related signal transductions (24). For example, direct neuronal death caused by JEV can be mediated by the (TNF) receptor-associated death domain (TRADD) protein (78), which thereupon regulates a downstream apoptotic cascade in neurons. It has been demonstrated that a TNF receptor-associated factor (TRAF), such as TRADD, can be regulated by caveolin-1 via direct association (20). Furthermore, the Src/Ras/extracellular signal-regulated kinase (ERK) signaling cascade, known to assemble on the caveolin scaffolds but not clathrin (29), was recently demonstrated to be involved in JEV-induced proinflammatory cytokine

expression, thus, causing neurotoxicity and indirect neuronal cell death (64). Therefore, caveola-mediated endocytosis may be required for specific signaling events that govern the severity of JEV pathogenesis.

In conclusion, we conducted a systematic study to identify the internalization mechanism of JEV in rat neuroblastoma cells. The evidence presented here indicates that JEV entry into B104 cells occurs by a pH-dependent, dynamin-dependent, and caveola-mediated endocytosis. Understanding the viral and cellular components involved in JEV invasion into the host cell, combined with a comprehension of the mechanisms that govern this process, should therefore open the possibility of developing new therapeutic approaches.

ACKNOWLEDGMENTS

We are grateful to Yong-Xin Yu (National Institute for the Control of Pharmaceutical and Biological Products, Beijing, China) for the JEV SA14 strain and Guo-Dong Liang (Center for Disease Control and Prevention, Fujian Province, China) for the isolated JEV strain SH-53.

This work was funded by the National Natural Science Foundation of China (30921006, 81171564), the Military S&T Project (AWS11C001), the National S&T Major Project for Infectious Diseases Control (2012ZX10004801-002-005), and the Shanghai Leading Academic Discipline Project (B901).

All authors have no conflicts of interest to disclose.

REFERENCES

1. **Acosta EG, Castilla V, Damonte EB.** 2008. Functional entry of dengue virus into Aedes albopictus mosquito cells is dependent on clathrin-mediated endocytosis. J. Gen. Virol. **89**:474–484.
2. **Acosta EG, Castilla V, Damonte EB.** 2009. Alternative infectious entry pathways for dengue virus serotypes into mammalian cells. Cell. Microbiol. **11**:1533–1549.
3. **Amstutz B, et al.** 2008. Subversion of CtBP1-controlled macropinocytosis by human adenovirus serotype 3. EMBO J. **27**:956–969.
4. **Ashok A, Atwood WJ.** 2003. Contrasting roles of endosomal pH and the cytoskeleton in infection of human glial cells by JC virus and simian virus 40. J. Virol. **77**:1347–1356.
5. **Benmerah A, Bayrou M, Cerf-Bensussan N, Dautry-Varsat A.** 1999. Inhibition of clathrin-coated pit assembly by an Eps15 mutant. J. Cell Sci. **112**:1303–1311.
6. **Boonsanay V, Smith DR.** 2007. Entry into and production of the Japanese encephalitis virus from C6/36 Cells. Intervirology **50**:85–92.
7. **Cantín C, Holguera J, Ferreira L, Villar E, Muñoz-Barroso I.** 2007. Newcastle disease virus may enter cells by caveolae-mediated endocytosis. J. Gen. Virol. **88**:559–569.
8. **Cao H, Thompson HM, Krueger EW, McNiven MA.** 2000. Disruption of Golgi structure and function in mammalian cells expressing a mutant dynamin. J. Cell Sci. **113**:1993–2002.
9. **Chien YJ, Chen WJ, Hsu WL, Chiou SS.** 2008. Bovine lactoferrin inhibits Japanese encephalitis virus by binding to heparan sulfate and receptor for low density lipoprotein. Virology **379**:143–151.
10. **Chu JJ, Ng ML.** 2004. Infectious entry of West Nile virus occurs through a clathrin-mediated endocytic pathway. J. Virol. **78**:10543–10555.
11. **Chu JJ, Ng ML.** 2004. Interaction of West Nile virus with alpha v beta 3 integrin mediates virus entry into cells. J. Biol. Chem. **279**:54533–54541.
12. **Chu JJ, Leong PW, Ng ML.** 2006. Analysis of the endocytic pathway mediating the infectious entry of mosquito-borne flavivirus West Nile into Aedes albopictus mosquito (C6/36) cells. Virology **349**:463–475.
13. **Clement C, et al.** 2006. A novel role for phagocytosis-like uptake in herpes simplex virus entry. J. Cell Biol. **174**:1009–1021.
14. **Coyne CB, Bergelson JM.** 2006. Virus-induced Abl and Fyn kinase signals permit coxsackievirus entry through epithelial tight junctions. Cell **124**:119–131.
15. **Damke H, Baba T, Warnock DE, Schmid SL.** 1994. Induction of mutant dynamin specifically blocks endocytic coated vesicle formation. J. Cell Biol. **127**:915–934.
16. **Das S, Laxminarayana SV, Chandra N, Ravi V, Desai A.** 2009. Heat shock protein 70 on Neuro2a cells is a putative receptor for Japanese encephalitis virus. Virology **385**:47–57.
17. **Das S, Chakraborty S, Basu A.** 2010. Critical role of lipid rafts in virus entry and activation of phosphoinositide 3′ kinase/Akt signaling during early stages of Japanese encephalitis virus infection in neural stem/progenitor cells. J. Neurochem. **115**:537–549.
18. **Doherty GJ, McMahon HT.** 2009. Mechanisms of endocytosis. Annu. Rev. Biochem. **78**:857–902.
19. **Eash S, Querbes W, Atwood WJ.** 2004. Infection of Vero cells by BK virus is dependent on caveolae. J. Virol. **78**:11583–11590.
20. **Feng X, et al.** 2001. Caveolin-1 associates with TRAF2 to form a complex that is recruited to tumor necrosis factor receptors. J. Biol. Chem. **276**:8341–8349.
21. **Fra AM, Williamson E, Simons K, Parton RG.** 1995. De novo formation of caveolae in lymphocytes by expression of VIP21-caveolin. Proc. Natl. Acad. Sci. U. S. A. **92**:8655–8659.
22. **Fujinaga Y, et al.** 2003. Gangliosides that associate with lipid rafts mediate transport of cholera and related toxins from the plasma membrane to endoplasmic reticulum. Mol. Biol. Cell **14**:4783–4793.
23. **Garuti R, et al.** 2005. The modular adaptor protein autosomal recessive hypercholesterolemia (ARH) promotes low density lipoprotein receptor clustering into clathrin-coated pits. J. Biol. Chem. **280**:40996–41004.
24. **Ghosh D, Basu A.** 2009. Japanese encephalitis—a pathological and clinical perspective. PLoS Negl. Trop. Dis. **3**:e437. doi:10.1371/journal.pntd.0000437.
25. **Ghoshal A, et al.** 2007. Proinflammatory mediators released by activated microglia induce neuronal death in Japanese encephalitis. Glia **55**:483–496.
26. **Gubler D, Kuno G, Markoff L.** 2007. Flaviviruses, p 1153–1252. *In* Knipe DM, Howley PM (ed), Fields virology, 5th ed, vol 1. Lippincott-Williams & Wilkins, Philadelphia, PA.
27. **Guo CJ, et al.** 2011. Entry of tiger frog virus (an Iridovirus) into HepG2 cells via a pH-dependent, atypical, caveolae-mediated endocytosis pathway. J. Virol. **85**:6416–6426.
28. **Harrison SC.** 2008. The pH sensor for flavivirus membrane fusion. J. Cell Biol. **183**:177–179.
29. **Hashimoto M, Takenouchi T, Rockenstein E, Masliah E.** 2003. Alpha-synuclein up-regulates expression of caveolin-1 and down-regulates extracellular signal-regulated kinase activity in B103 neuroblastoma cells: role in the pathogenesis of Parkinson's disease. J. Neurochem. **85**:1468–1479.
30. **Johannsdottir HK, Mancini R, Kartenbeck J, Amato L, Helenius A.** 2009. Host cell factors and functions involved in vesicular stomatitis virus entry. J. Virol. **83**:440–453.
31. **Krishnan MN, et al.** 2007. Rab 5 is required for the cellular entry of dengue and West Nile viruses. J. Virol. **81**:4881–4885.
32. **Lau AW, Chou MM.** 2008. The adaptor complex AP-2 regulates post-endocytic trafficking through the non-clathrin Arf6-dependent endocytic pathway. J. Cell Sci. **121**:4008–4017.
33. **Le PU, Nabi IR.** 2003. Distinct caveolae-mediated endocytic pathways target the Golgi apparatus and the endoplasmic reticulum. J. Cell Sci. **116**:1059–1071.
34. **Lee CJ, Lin HR, Liao CL, Lin YL.** 2008. Cholesterol effectively blocks entry of flavivirus. J. Virol. **82**:6470–6480.
35. **Lee CJ, Liao CL, Lin YL.** 2005. Flavivirus activates phosphatidylinositol 3-kinase signaling to block caspase-dependent apoptotic cell death at the early stage of virus infection. J. Virol. **79**:8388–8399.
36. **Macia E, et al.** 2006. Dynasore, a cell-permeable inhibitor of dynamin. Dev. Cell **10**:839–850.
37. **Marechal V, et al.** 2001. Human immunodeficiency virus type 1 entry into macrophages mediated by macropinocytosis. J. Virol. **75**:11166–11177.
38. **Marjomaki V, et al.** 2002. Internalization of echovirus 1 in caveolae. J. Virol. **76**:1856–1865.
39. **Marsh M, Helenius A.** 2006. Virus entry: open sesame. Cell **124**:729–740.
40. **Mayor S, Pagano RE.** 2007. Pathways of clathrin-independent endocytosis. Nat. Rev. Mol. Cell Biol. **8**:603–612.
41. **McMinn PC.** 1997. The molecular basis of virulence of the encephalitogenic flaviviruses. J. Gen. Virol. **78**:2711–2722.
42. **Medigeshi GR, Hirsch AJ, Streblow DN, Nikolich-Zugich J, Nelson JA.** 2008. West Nile virus entry requires cholesterol-rich membrane microdomains and is independent of alphavbeta3 integrin. J. Virol. **82**:5212–5219.
43. **Mineo C, Ying YS, Chapline C, Jaken S, Anderson RG.** 1998. Targeting of protein kinase Calpha to caveolae. J. Cell Biol. **141**:601–610.

44. **Misra UK, Kalita J.** 2010. Overview: Japanese encephalitis. Prog. Neurobiol. **91**:108–120.
45. **Mizzen L, Hilton A, Cheley S, Anderson R.** 1985. Attenuation of murine coronavirus infection by ammonium chloride. Virology **142**:378–388.
46. **Mosso C, Galván-Mendoza IJ, Ludert JE, del Angel RM.** 2008. Endocytic pathway followed by dengue virus to infect the mosquito cell line C6/36 HT. Virology **378**:193–199.
47. **Mukhopadhyay S, Kuhn RJ, Rossmann MG.** 2005. A structural perspective of the flavivirus life cycle. Nat. Rev. Microbiol. **3**:13–22.
48. **Nawa M, Machida S, Takasaki T, Kurane I.** 2007. Plaque formation by Japanese encephalitis virus bound to mosquito C6/36 cells after low pH exposure on the cell surface. Jpn. J. Infect. Dis. **60**:118–120.
49. **Nawa M, Takasaki T, Yamada K, Kurane I, Akatsuka T.** 2003. Interference in Japanese encephalitis virus infection of Vero cells by a cationic amphiphilic drug, chlorpromazine. J. Gen. Virol. **84**:1737–1741.
50. **Nelson N.** 2003. A journey from mammals to yeast with vacuolar H^+-ATPase (V-ATPase). J. Bioenerg. Biomembr. **35**:281–289.
51. **Nomura R, Fujimoto T.** 1999. Tyrosine-phosphorylated caveolin-1: immunolocalization and molecular characterization. Mol. Biol. Cell **10**:975–986.
52. **Nunes-Correia I, Eulálio A, Nir S, Pedroso de Lima MC.** 2004. Caveolae as an additional route for influenza virus endocytosis in MDCK cells. Cell. Mol. Biol. Lett. **9**:47–60.
53. **Oh P, McIntosh DP, Schnitzer JE.** 1998. Dynamin at the neck of caveolae mediates their budding to form transport vesicles by GTP-driven fission from the plasma membrane of endothelium. J. Cell Biol. **141**:101–114.
54. **Parton RG, Joggerst B, Simons K.** 1994. Regulated internalization of caveolae. J. Cell Biol. **127**:1199–1215.
55. **Patel KP, Coyne CB, Bergelson JM.** 2009. Dynamin- and lipid raft-dependent entry of decay-accelerating factor (DAF)-binding and non-DAF-binding coxsackieviruses into nonpolarized cells. J. Virol. **83**:11064–11077.
56. **Pelkmans L, Helenius A.** 2003. Insider information: what viruses tell us about endocytosis. Curr. Opin. Cell Biol. **15**:414–422.
57. **Pelkmans L, Püntener D, Helenius A.** 2002. Local actin polymerization and dynamin recruitment in SV40-induced internalization of caveolae. Science **296**:535–539.
58. **Pelkmans L, et al.** 2005. Genome-wide analysis of human kinases in clathrin- and caveolae/raft-mediated endocytosis. Nature **436**:78–86.
59. **Pelkmans L, Kartenbeck J, Helenius A.** 2001. Caveolar endocytosis of simian virus 40 reveals a new two-step vesicular-transport pathway to the ER. Nat. Cell Biol. **3**:473–483.
60. **Perry JW, Wobus CE.** 2010. Endocytosis of murine norovirus 1 into murine macrophages is dependent on dynamin II and cholesterol. J. Virol. **84**:6163–6176.
61. **Pitha J, Irie T, Sklar PB, Nye JS.** 1988. Drug solubilizers to aid pharmacologists: amorphous cyclodextrin derivatives. Life Sci. **43**:493–502.
62. **Rahn E, Petermann P, Hsu MJ, Rixon FJ, Knebel-Mörsdorf D.** 2011. Entry pathways of herpes simplex virus type 1 into human keratinocytes are dynamin- and cholesterol-dependent. PLoS One **6**:e25464. doi:10.1371/journal.pone.0025464.
63. **Raung SL, Kuo MD, Wang YM, Chen CJ.** 2001. Role of reactive oxygen intermediates in Japanese encephalitis virus infection in murine neuroblastoma cells. Neurosci. Lett. **315**:9–12.
64. **Raung SL, Chen SY, Liao SL, Chen JH, Chen CJ.** 2007. Japanese encephalitis virus infection stimulates Src tyrosine kinase in neuron/glia. Neurosci. Lett. **419**:263–268.
65. **Sancey L, et al.** 2009. Clustering and internalization of integrin alphavbeta3 with a tetrameric RGD-synthetic peptide. Mol. Ther. **17**:837–843.
66. **Sanchez A.** 2007. Analysis of filovirus entry into Vero e6 cells, using inhibitors of endocytosis, endosomal acidification, structural integrity, and cathepsin (B and L) activity. J. Infect. Dis. **196**:S251–S258.
67. **Sánchez-San Martín C, López T, Arias CF, López S.** 2004. Characterization of rotavirus cell entry. J. Virol. **78**:2310–2318.
68. **Sandvig K, Torgersen ML, Raa HA, van Deurs B.** 2008. Clathrin-independent endocytosis: from nonexisting to an extreme degree of complexity. Histochem. Cell Biol. **129**:267–276.
69. **Schelhaas M.** 2010. Come in and take your coat off—how host cells provide endocytosis for virus entry. Cell. Microbiol. **12**:1378–1388.
70. **Sieczkarski SB, Whittaker GR.** 2002. Influenza virus can enter and infect cells in the absence of clathrin-mediated endocytosis. J. Virol. **76**:10455–10464.
71. **Sieczkarski SB, Whittaker GR.** 2002. Dissecting virus entry via endocytosis. J. Gen. Virol. **83**:1535–1545.
72. **Silva MC, Guerrero-Plata A, Gilfoy FD, Garofalo RP, Mason PW.** 2007. Differential activation of human monocyte-derived and plasmacytoid dendritic cells by West Nile virus generated in different host cells. J. Virol. **81**:13640–13648.
73. **Simons K, Toomre D.** 2000. Lipid rafts and signal transduction. Nat. Rev. Mol. Cell Biol. **1**:31–39.
74. **Sorkin A, von Zastrow M.** 2009. Endocytosis and signalling: intertwining molecular networks. Nat. Rev. Mol. Cell Biol. **10**:609–622.
75. **Suksanpaisan L, Susantad T, Smith DR.** 2009. Characterization of dengue virus entry into HepG2 cells. J. Biomed. Sci. **16**:17. doi:10.1186/1423-0127-16-17.
76. **Sun X, Yau VK, Briggs BJ, Whittaker GR.** 2005. Role of clathrin-mediated endocytosis during vesicular stomatitis virus entry into host cells. Virology **338**:53–60.
77. **Superti F, et al.** 1987. Entry pathway of vesicular stomatitis virus into different host cells. J. Gen. Virol. **68**:387–399.
78. **Swarup V, Ghosh J, Das S, Basu A.** 2008. Tumor necrosis factor receptor-associated death domain mediated neuronal death contributes to the glial activation and subsequent neuroinflammation in Japanese encephalitis. Neurochem Int. **52**:1310–1321.
79. **Tani H, et al.** 2010. Involvement of ceramide in the propagation of Japanese encephalitis virus, J. Virol. **84**:2798–2807.
80. **Tani H, et al.** 2007. Replication-competent recombinant vesicular stomatitis virus encoding hepatitis C virus envelope proteins. J. Virol. **81**:8601–8612.
81. **Thomsen P, Roepstorff K, Stahlhut M, van Deurs B.** 2002. Caveolae are highly immobile plasma membrane microdomains, which are not involved in constitutive endocytic trafficking. Mol. Biol. Cell **13**:238–250.
82. **Urs NM, et al.** 2005. A requirement for membrane cholesterol in the beta-arrestin- and clathrin-dependent endocytosis of LPA1 lysophosphatidic acid receptors. J. Cell Sci. **118**:5291–5304.
83. **van der Schaar HM, et al.** 2008. Dissecting the cell entry pathway of dengue virus by single-particle tracking in living cells. PLoS Pathog. **4**:e1000244. doi:10.1371/journal.ppat.1000244.
84. **Wang LH, Rothberg KG, Anderson RG.** 1993. Mis-assembly of clathrin lattices on endosomes reveals a regulatory switch for coated pit formation. J. Cell Biol. **123**:1107–1117.
85. **West MA, Bretscher MS, Watts C.** 1989. Distinct endocytotic pathways in epidermal growth factor-stimulated human carcinoma A431 cells. J. Cell Biol. **109**:2731–2739.
86. **Wu SC, Chiang JR, Lin CW.** 2004. Novel cell adhesive glycosaminoglycan-binding proteins of Japanese encephalitis virus. Biomacromolecules **5**:2160–2164.
87. **Zhu YZ, et al.** 2012. Association of heat-shock protein 70 with lipid rafts is required for Japanese encephalitis virus infection in Huh7 cells. J. Gen. Virol. **93**:61–71.